HOMODIMER AND HETERODIMER SYNTHESIS OF MACROCYCLES CONTAINING 2-AMINOOCTANOIC ACID, LYSINE AND SERINE

by

Gretchen M. Pavelich

Submitted in partial fulfillment of the

requirements for Departmental Honors in

the Department of Chemistry and Biochemistry

Texas Christian University

Fort Worth, Texas

December 11, 2023

HOMODIMER AND HETERODIMER SYNTHESIS OF MACROCYCLES CONTAINING 2-AMINOOCTANOIC ACID, LYSINE AND SERINE

Project Approved

Supervising Professor: Eric Simanek Ph.D.

Department of Chemistry and Biochemistry

Sergei Dzyuba Ph.D.

Department of Chemistry and Biochemistry

Mikaela Stewart Ph.D.

Department of Biology

Abstract

Increasingly, pharmaceutical companies focus on developing orally available drugs because they offer ease of administration and improve patient compliance. A drug achieves oral availability by possessing a hydrophilic and a hydrophobic component, allowing it to partition across the membrane. A key parameter for evaluating the oral availability, logP, is determined by the compound's partitioning between oil and water, typically measured using RP-HPLC. Orally available drugs have a logP between -0.4 and 5. Towards this goal, we explored the possibility of tuning logP values by modulating the structure of the synthetic macrocycles.

This thesis explores the syntheses of 24-atom macrocycles with contrasting polarities as a potential model for developing orally available drugs. A three-step process is employed to make macrocycles. First, cyanuric chloride is sequentially substituted with BOC-hydrazine, then an amino acid, and finally, dimethylamine, to yield **X-acid**, where **X** represents an amino acid. Next, an acetal group is added to form the monomer, **X-M**. Under acidic conditions, hydrogen bonding templates the dimerization of two monomers, forming the macrocycle **X-X.**

The macrocycle achieves differing polarities by incorporating various amino acids into the scaffolds. The hydrophobic component of the heterodimer is achieved with 2-aminooctanoic acid (**OA**), characterized by its long hydrocarbon chain, while serine and lysine represent the hydrophilic component. NMR spectroscopy distinguishes and analyzes the new resonances of the heterodimers **OA-K** and **OA-S**. The polarity of the heterodimers was analyzed with RP-HPLC and TLC and compared to the corresponding homodimers. The conclusion of this work is that the logP of macrocycles can be tuned through the synthesis of heterodimers.

Acknowledgments

I want to express my heartfelt gratitude to everyone who played a pivotal role in helping me turn my ambitious, freshman dream of writing an honors thesis into reality. First and foremost, I want to thank Dr. Eric Simanek for welcoming me into his lab and providing a source of guidance throughout this entire process. I extend my sincere thanks to Drs. Sergei Dzyuba and Mikaela Stewart for serving on my committee. A special shout-out goes to Casey Patterson-Gardner and Alex Menke, who provided information for this thesis and answered my questions…well, sometimes. To all the professors within the Department of Chemistry and Biochemistry, I wish to thank each of you individually, but that would turn into a 50-page thesis. Despite the challenges posed by the curriculum, I genuinely appreciated the opportunity to engage with your material, and more importantly, get to know each of you better. It was a two-for-one deal. Thank you to my family for allowing me to pursue something that makes no sense to them. Hopefully, this thesis will clear things up. Lastly, thank you to the John V. Roach Honors College and the College of Science and Engineering for this opportunity to make my dream a reality. Financially, this research was supported by the Texas Christian University through a grant for undergraduate research (SERC-UG-200707), the National Institutes of Health, and the Robert A. Welch Foundation.

Table of Contents

Terminology and Abbreviations

Abbreviation	Term
BOC	tert-butyloxycarbonyl
C	carbon
CC	cyanuric chloride
COSY	homonuclear correlation spectroscopy
Da	Daltons
DCM	dichloromethane
DIPEA	N,N-diisopropylethylamine
DMA	dimethylamine
DMSO	dimethylsulfoxide
ESI	electrospray ionization
H	hydrogen
HBTU	hexafluorophosphate benzotriazole tetramethyl uronium
HCl	hydrochloric acid
HOBT	hydroxybenzotriazole
HPLC	high performance liquid chromatography
HRMS	high resolution mass spectrometry
K	lysine
logP	log of partition coefficient
MeOH	methanol

NaOH	sodium hydroxide
NMR	nuclear magnetic resonance spectroscopy
OA	2-aminooctanoic acid
ppm	parts per million
Rf	retention factor
rOsey	rotating frame Overhauser effect spectroscopy
Ro5	rule of 5
RP-HPLC	reverse phase high performance liquid chromatography
Rt	retention time
S	serine
TFA	trifluoracetic acid
THF	tetrahydrofuran
TLC	thin layer chromatography
TMU	tetramethyl urea
UV	ultraviolet
X	arbitrary amino acid

Charts, Figures, and Schemes

Introduction

Compared to those administered by injection, orally available drugs provide a significant advantage in patient convenience and compliance.[1] The challenges of achieving oral availability lie in creating a drug that possesses both aqueous solubility and membrane permeability.[2] Aqueous solubility is needed to reach the cellular target and navigate the intracellular space. Hydrophobic characteristics are needed to partition through the membrane and cross from one aqueous compartment to the other.[3] If a potential drug is too hydrophilic (water-loving), it can travel through the GI tract or vasculature but would not pass through membranes due to polarity differences. On the other hand, if a drug is too hydrophobic, it cannot travel through the GI tract or vasculature and instead would be imprisoned in a hydrophobic domain such as fat or bound to circulating protein (**Figure 1**).

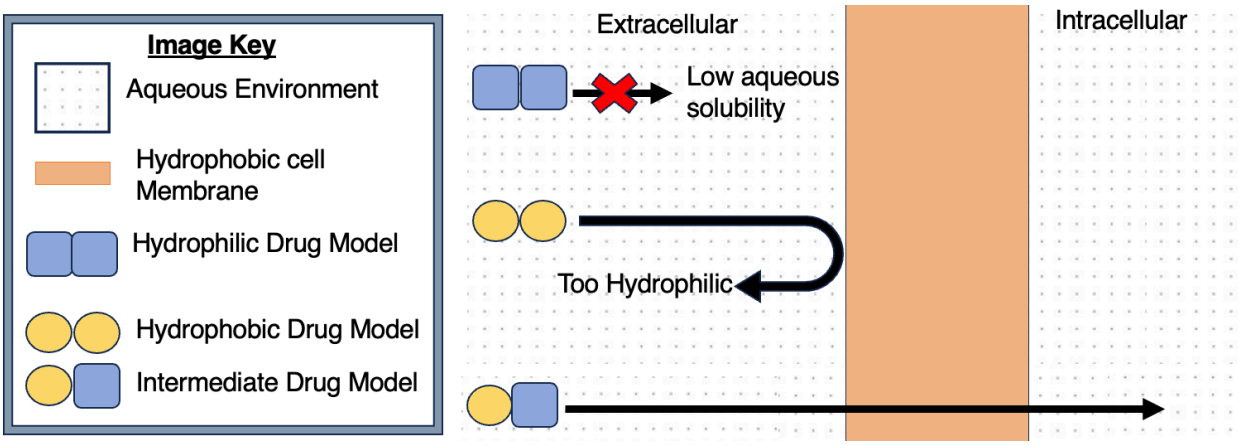

Figure 1. Drugs with both hydrophobic and hydrophilic chemical properties indicated as "intermediate drug model" are able to gain access to the membrane, facilitate through, and have an intracellular target.

One way to predict drug oral availability is to apply Lipinski's rule of five, Ro5.[4] The Ro5 stipulates that for an oral drug to be orally available, it should meet the following criteria: a

maximum of five hydrogen bond donors, a maximum of 10 hydrogen bond acceptors, a molecular mass less than 500 Da, and a logP that does not exceed five.[4] These rules established strict criteria for potential drugs and guided the pharmaceutical industry for decades.[5] More recently, however, there has been a focus on examining molecules outside the Ro5 to increase the library of potential orally available compounds. Currently, there is a strong focus on larger molecules, such as macrocycles with a molecular weight exceeding 500 Da, which fall outside the conventional Ro5.[6]

Macrocycles are cyclic molecules with more than twelve atoms bonded in a ring.[7] The advantage of their larger size is that they can access a different therapeutic paradigm. Instead of blocking an active site like a small molecule drug, these molecules are large enough to interfere with protein-protein interactions. Cyclosporine, an immunosuppressant medication for an organ transplant, exemplifies a macrocyclic drug. Cyclosporine is a natural product composed of a peptide ring with 33 atoms.[8] Cyclosporine has a molecular weight greater than 500 Da and thus exists beyond the rule of 5, but is administered orally. Other orally available drugs existing outside the Ro5 include vancomycin, erythromycin, and rapamycin. The lesson that emerges is that Nature creates bioactive macrocycles outside the Ro5. Now, the pharmaceutical industry is starting to follow and utilizes the Ro5 to mimic Nature.

This thesis focuses on synthesizing the 24-atom triazine macrocycles through a simple, three-step process (**Scheme 1**). The monomer, **X-M**, is synthesized by starting with cyanuric chloride, CC, which undergoes three nucleophilic aromatic substitution reactions with BOC-hydrazine, an amino acid (**X**), and dimethylamine, DMA, to obtain the acid, **X-acid**. Adding the acetal to the carboxylic acid group of the amino acid to produce **X-M** is accomplished using coupling reagents. The final

step involves placing **X-M** in an acidic solution and allowing the solvent to evaporate, forming a macrocycle, **X-X**, without purification.[9] The acidic solution of trifluoracetic acid, TFA, facilitates reaction and hydrogen-bonded templating, where the protonated triazine ring on one monomer interacts with the carbonyl of the amide on the other monomer.[10] Thus, the two monomers come together via a hydrogen bonded network where the proton is important for the two monomers to come together.

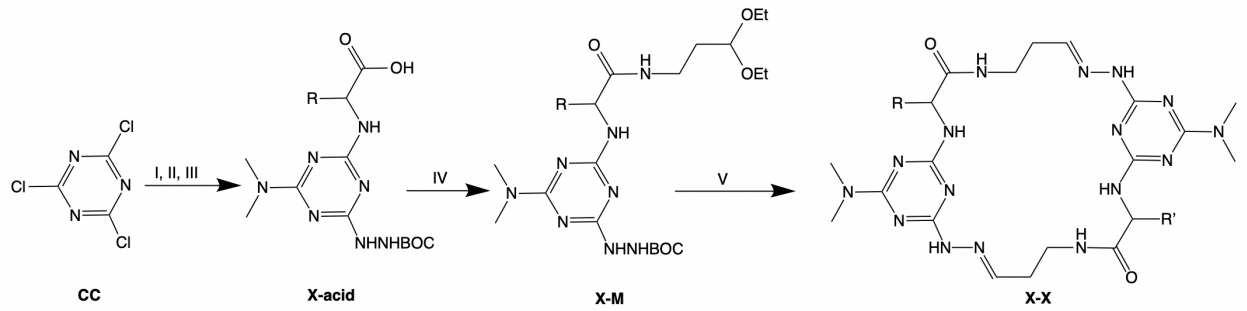

Scheme 1. Synthesis of macrocycle. I) BOC-hydrazine, NaOH (aq), THF. II) amino acid. III) DMA. IV) DIPEA, HBTU, HOBT and 1-amino-3,3-didethylpropane. V) DCM : TFA (1:1).

While **Scheme 1** shows two identical monomers coming together (so-called homodimers), this work explores synthesizing and characterizing macrocycles that incorporate two different monomers into a structure known as a heterodimer.

> *We hypothesize that heterodimers with two different amino acids, one being hydrophobic and the other hydrophilic, will lead to the emergence of chemical properties that are intermediate to corresponding homodimers.*

The hydrophobic amino acid chosen for this study is 2-aminooctanoic acid, **OA**, an unnatural amino acid featuring a substantially long hydrocarbon chain (**Chart 1**). The two hydrophilic amino acids used in this research are lysine, **K**, and serine, **S**. Lysine is an essential amino acid characterized by a primary amine attached to a hydrocarbon chain, while **S** is a nonessential amino

acid containing a primary alcohol group. Both **S** and **K** have a nucleophile that researchers can modify for further investigation. The heterodimers targeted for synthesis and characterization in this study are **OA-S** and **OA-K**.

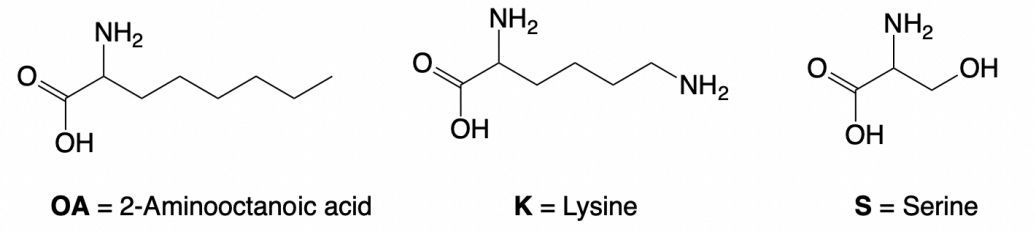

Chart 1. Chemical structures of amino acids **OA**, **K** and **S**.

The physical property that we have chosen to evaluate the hypothesis is polarity. The polarity of the heterodimers will be measured using thin-layer chromatography (TLC) and reverse-phase high-performance liquid chromatography (RP-HPLC). Thin-layer chromatography is a separation technique in which the compound's polarity dictates how far it migrates on a stationary phase as a function of the nature of the stationary and mobile phase. Here, the stationary phase is polar, with silica attached to a glass slide referred to as a plate. When this plate with absorbed mixture of compounds is placed in an eluent (known as mobile phase), the mixture moves up the plate due to specific capillary action, thus leading to separation the compounds by affinities for the eluent and the silica. The retention factor (Rf) is the distance traveled by the sample over the distance traveled by the solvent. In comparison, the Rf value that is closer to one represents a more hydrophobic compound and the lower one a more hydrophilic compound. The Rf is measured in the absence of controls. It is the result of a formula and is dependent on the eluent and stationary phase. Two applications in this research utilize TLC: first, to monitor the progress of the reactions, and second to test the hypothesis about the polarity of novel macrocycles.

Similar to TLC, RP-HPLC offers a solid support (a stationary phase) that interacts with the molecules. The stationary phase contains long hydrocarbon chains (ex. C18) to model the cell membrane. Unlike the polar silica phase of TLC, hydrophobic molecules experience longer retention than hydrophilic ones. Here, one can adjust the pH of the eluent, which is a solution of methanol (MeOH) and water. By comparing the retention time of the molecule with standards having known logPs, one can determine a logP. LogP is the logarithm of the ratio of molecules that partition between the organic and aqueous phases. LogP denotes neutral molecules, while logD is used to convey that the measurement was done on charged molecules. Historically, logP was determined by measuring the relative distributions of the molecule in a mixture of octanol and water. Methods relying on RP-HPLC, however, are quicker and simpler to execute. Drug makers try to ensure that the molecules of interest have logP values between -0.4 and 5 in certain pH conditions. Ghose established the lower bound for logP, while Lipinski defined the upper bound.[11]

Both methods can evaluate the polarity of the molecules. However, RP-HPLC can be used to determine the logP of the molecules of interest more accurately and reproducibly. Thin-layer chromatography is helpful because it is a quicker method to determine the distribution of products due to polarity. Both methods evaluate different aspects of polarity between products, but RP-HPLC is the method to determine logP.

The work described in this thesis is divided into five parts. Part 1 describes the synthesis of monomers **S-M** and **OA-M**. In part 2, homodimers, **OA-OA**, **S-S,** and **K-K** are described and characterized by structural analysis. Part 3 describes the synthesis and structural analysis of the heterodimers **OA-S** and **OA-K**. Part 4 focuses on the shape of the **OA-OA** macrocycle. Part 5

addresses the guiding hypothesis that the heterodimers show properties intermediate to homodimers using both TLC and RP-HPLC.

Experimental

Materials & Methods. All reagents and solvents were purchased from commercial sources and used as received. The TLC experiments were visualized with ultraviolet light, UV, or stained with ninhydrin (1.5g ninhydrin in 100 mL of n-butanol and 3.0 mL acetic acid), followed by heating. The chromatographic separations were carried out on silica gel (Silicycle) with a porosity of 60Å, particle size of 50 to 63 μm, surface area of 500 to 600 m^2/g, a bulk density of 0.4 g/mL, and a pH range of 6.5 to 7.5. The eluent for the chromatographic purification contained different ratios of dichloromethane (DCM) and MeOH. Excess solvents were removed using rotary evaporation on a Buchi Rotovapor RII with a Welch Self-Cleaning Dry Vacuum System. All workup and purification procedures were conducted with reagent-grade solvents under an ambient atmosphere.

NMR Spectroscopy. All NMR spectra were recorded with a 400 MHz Bruker Avance spectrometer. The chemical shifts in the ^{1}H and ^{13}C spectra were calibrated to the corresponding residual solvent resonance in parts per million, ppm.

RP-HPLC Determination of logP and logD by Retention Time. An acidic eluent was prepared with 750 mL of reagent grade MeOH and 250 mL of ultrapure water (18.2 mohms, Thermo Scientific Smart2 Pure 3). The eluent was degassed for 2 hours with a sonicator, and then 1 mL TFA was added to the eluent, bringing the pH to about 2. Samples and standards for RP-HPLC were prepared at a concentration of 2 mM solutions in 1 mL of the eluent solvent within a vial or by adding a drop from an NMR sample when solid, dry sample was unavailable. Samples were filtered through

a syringe filter (PTFE, 0.45 μm diameter) to remove any precipitate due to limited solubility in the eluent before running with a HPLC. Before running the samples, the HPLC system was purged with eluent for 20 minutes to ensure the absence of air bubbles or other eluents in the system. Nine controls were run with an increase in hydrophobicity, followed by with a wash of the eluent for the injector needle used after. The HPLC traces of samples/standards were acquired using the following parameters: 1.0 μL injection volume (0.5 μL for the third trial), 0.2 mL/min flow rate, and 254.4 nm detection.

The logP values for **OA-OA**, **B OA-K,** and **B K-K** correspond to neutral species. The logD values of **OA-OA**, **OA-S,** and **S-S** correspond to ionized species.

The Rt for each standard in the **B OA-K** mixture was converted into a K-value by subtracting the lysine Rt (the dead volume standard) and then dividing the difference by the lysine Rt. For the **OA-S** mixture the dead volume standard used for the calculations was serine's Rt. Next, the logK for each value was determined by taking the log of each K-value. A graph of known logP for the standards vs logK was constructed (**B OA-K Graph 1, OA-S Graph 2**). Values for all standards associated with **B OA-K** are seen in the supporting information (**Chart S1**). Values for all standards associated with **OA-S** are seen in the supporting information (**Chart S2**). The macrocycles' primary amines associated with amino acid side chain **L** were acylated prior to logP determination. Thus, the equation logP= 3.794 (logK) + 2.22, with a R^2 value of 0.992, takes the measured logK of **OA-OA**, **B OA-K,** and **B K-K** and converts them into their logP from the Rt determined by HPLC. The logP for **OA-OA**, **B OA-K** and **B K-K** was 5.4, 3.8, and 2.6, respectively, see **Table 1** for their Rt, k-value, and logK. The equation for the **OA-S** was logD =

0.3298 (logK) – 1.0195 with a R^2 of 0.994. The logD values for **OA-OA**, **OA-S** and **S-S** are 4.2, 0.8 and < -2.2, respectively, and see **Table 2** for their Rt, k-value, and logK.

X-acid. Cyanuric chloride (0.370g, 2 mmol) was dissolved in 7.4 mL of tetrahydrofuran, THF, chilled to 0°C with an ice bath. BOC-hydrazine (0.264g, 2 mmol) was dissolved in 7.4 mL of THF and then added dropwise to the solution. During the addition, the solution turned yellow. After the addition was completed, 2 mL of 1M sodium hydroxide, NaOH, (2 mmol) was added dropwise. The yellow color faded to a cloudy white. After 30 minutes, a TLC (5% MeOH in DCM, spot visualization done by UV) showed the presence of a single spot (Rf: 0.8), which was yellow by ninhydrin stain, thus indicating the completion of the first step. Next, the solution was warmed to room temperature before the addition of the amino acids.

The amino acid **OA** (0.317g, 2 mmol) was added. Upon addition, the solution turned bright yellow and had a pH of 11. After 1 hr, the reaction was too basic, and drops of 1 M hydrochloric acid, HCl, were added until the pH was 9. One hour later, TLC (5% MeOH in DCM) showed the disappearance of the starting material (Rf: 0.8) and the formation of a new spot (Rf: 0.5).

In the other flask, **S** (0.326g, 2.02 mmol) was slowly added with 1 equivalent of water (3 mL). After addition, the pH was 8, and the solution had a yellow color. After 6 hrs, TLC (5% MeOH in DCM) showed the disappearance of the starting material (Rf: 0.8) and the formation of a new spot (Rf: 0.4).

An aqueous solution of 40% DMA was added dropwise to the reaction flasks. (DMA in **OA** 0.456 g, 4 mmol; DMA in **S** 0.457g, 4 mmol) The pH went from a 4 to a 9. After 2 hrs, drops of 1 M NaOH were added to bring the pH up to 10. The color changed from cloudy yellow to cloudy white. After 24 hrs, TLC (10% MeOH in DCM) showed a new spot at Rf: 0.4. The solution was acidified to a pH of 4 with 1M HCl. Then, the reaction mixture was diluted with 50 mL of brine and extracted with 25 mL of ethyl acetate. The organic layer dried over magnesium, and the organic solution was removed with rotovap. The resulting residue was subjected to silica gel column chromatography (10% MeOH in DCM), to give **OA-acid** (0.0.247 g, 30%). ^{1}H NMR (DMSO-d_6, 400 MHz): δ 8.53 – 8.42 (m, 1 H), 8.25 – 8.01 (m, 1 H), 6.25 (bs, 1 H), 4.12 (s, 1 H), 3.00 (s, 6 H), 1.70 (m, 2 H), 1.44 – 1.11 (m, 17 H), 0.83 (m, 3 H). ^{13}C{^{1}H} NMR (DMSO-d_6, 100 MHz): δ 174.6, 162.1, 153.5, 153.4, 146.9, 55.4, 363.3, 36.0, 33.6, 31.6, 31.3, 28.7, 25.2, 22.2, 13.0.

The resulting silica gel column for the **S-acid** had fractions with two spots by TLC (Rf: 5 and 8). Then, later fractions had only one spot (Rf: 5). The impurities within the sample had two spots by TLC. When proceeding to the next step, the two reactions were separated. The yield of **S-acid** was 0.210 g (30%). ^{1}H NMR for **S-acid** (DMSO-d_6, 400 MHz): δ 8.48 – 8.04 (m, 1 H), 5.98 – 9.95 (m, 1 H), 4.24 (s, 1 H), 3.68 – 3.65 (m, 2 H), 2.99 (s, 6 H), 1.40 – 1.23 (m, 9 H), 1.06 (m, 9H).

X-Monomer. The **OA-acid** dissolved in 6 mL of DCM. Then, reagents were added sequentially, starting with N,N-diisopropylethylamine (DIPEA, 0.187g, 1.44 mmol), then HBTU (0.277g, 1.44 mmol), followed by HOBT (0.0987g, 0.73 mmol) and lastly, 1-amino-3,3-didethylpropane (0.0988g, 0.74 mmol). The color of the reaction mixture changed throughout the addition from

colorless to clear yellow. The pH was 9. After 1 hr, the pH was 4, and a TLC (10% MeOH in DCM) showed no new spots by UV; one equivalent of DIPEA was added (0.0799g, 0.60 mmol) and in one hour TLC (10% MeOH in DCM) showed a new spot at Rf: 0.6. After 1 hr, the solution was brought to a pH of 4 with 1 M HCl. Then, the reaction mixture was diluted with 50 mL of brine and extracted with 25 mL of ethyl acetate. The organic layer was dried with magnesium sulfate, and after removal of ethyl acetate, the residue was subjected to silica gel column chromatography (5% MeOH in DCM), to yield 0.147g of pure product (45% yield). ^{1}H NMR (DMSO-d_6, 400 MHz): δ 8.51 (m, 1 H), 8.38 – 8.04 (m, 1 H), 7.77 – 7.48 (m, 1 H), 6.71 – 6.49 (m, 1H), 4.43 (m, 1 H), 4.32 – 4.16 (m, 1 H), 3.52 (m, 2 H), 3.37 (m, 2 H), 3.07 (m, 2 H), 2.99 (m, 6 H), 1.69 – 1.52 (m, 4 H), 1,44 – 1.14 (m, 17 H), 1.08 (m, 6 H), 0.84 (m, 3 H). ^{13}C {1H} NMR (DMSO-d_6, 100 MHz): δ 172.7, 172.6, 165.6, 165.3, 156.1, 155.7, 100.52, 78.55, 60.8, 59.8, 54.9, 54.5, 35.4, 34.7, 33.4, 32.0, 31.2, 28.5, 28.2, 25.5, 22.0, 15.3, 14.1, 14.0.

The same procedure was followed for the pure and impure **S-acid**. Pure **S-acid**, 0.094 g, dissolved in 2.27 mL of DCM. Then the following were added in sequence: DIPEA (0.0730 g 0.56), HBTU (0.104 g, 0.27 mmol), HOBT (0.0372 g, 0.027 mmol), and lastly 1-amino-3,3-didethylpropane (0.0317 g 0.24 mmol). After the addition, the reaction mixture had a pH of 8. Impure **S-acid** dissolved in DCM. The following were added in succession: DIPEA (0.0877 g, 0.68 mmol), HBTU (0.129 g, 0.34 mmol), HOBT (0.0385 g, 0.28 mmol), and finally 1-amino-3,3-didethylpropane (0.0317 g 0.24 mmol). The reaction mixture had a pH of 8. TLC (10% MeOH in DCM) showed that both products had a spot at Rf: 0.7. The two monomers were mixed and diluted with 50 mL of brine and extracted ethyl acetate. Magnesium sulfate dried the organic layer. After removal of ethyl acetate, the residue was subjected to silica gel column chromatography (5% MeOH in DCM)

was used to isolate the monomer, and the **S-M** yield was 0.0618 g (22% yield). ^{1}H NMR (DMSO-d_6, 400 MHz): δ 8.62 – 8.07 (m, 1 H), 7.78 – 7.61 (m, 1 H), 6.25 – 6.13 (m, 1 H), 4.46 (m, 1 H), 4.37 (m, 1 H), 3.55 – 3.46 (m, 2 H), 3.41 – 3.37 (m, 2 H), 3.11 – 3.06 (m, 2 H), 3.00 (m, 6 H), 1.64 (m, 2 H), 1.40 – 1.23 (m, 9 H), 1.11 – 1.04 (m, 15 H). ^{13}C {^{1}H} NMR (DMSO-d_6, 100 MHz): δ 170.5, 167.6, 167.3, 165.3, 164.6, 155.9, 100.5, 78.5, 72.7, 62.1, 61.9, 60.8, 60.7, 55.1, 54.5, 54.2, 38.2, 35.4, 34.8, 33.3, 28.2, 27.2, 27.1, 15.3.

Homodimer Macrocycles. The **X-M** (**OA-M** 0.062g, 0.11 mmol, **S-M** 0.0179g, 0.03 mmol) dissolved in 1 mL of DCM in a vial with a stir bar. Then 1 mL of TFA was slowly added dropwise. The solution was allowed to evaporate within a hood, which took 72 hrs for the **OA-OA** vial and one week for the **S-S** vial. The **S-S** vile never fully evaporated. The resulting macrocycles, **OA-OA** and **S-S**, were analyzed by NMR to verify structure and purity. By TLC, **OA-OA** had one spot (Rf: 0.7), indicating all the monomers reacted to form a macrocycle. In the ^{1}H NMR spectrum for **OA-OA**, successful macrocycle synthesis is established with the appearance of NNH and A at 12.49 ppm and 7.46 ppm, respectively. The ^{13}C NMR spectrum is consistent with macrocycle formation with the A resonance at 148.9 ppm. **OA-OA** spectra: ^{1}H NMR (DMSO-d_6, 400 MHZ): δ 12.49 (s, 1 H), 11.67 (s, 1.H), 9.10 (m**,** 1 H), 7.69 (m, 1 H), 7.46 (s, 1 H), 4.28 (m, 1 H), 4.05 (m, 1 H), 3.11 – 3.03 (m, 1 H), 3.10 (s, 3 H), 3.06 (s, 3 H), 2.69 – 2.52 (m, 2 H), 1.73 (m, 2 H), 1.51 – 1.19 (m, 8 H), 0.86 (m, 3 H). ^{13}C {^{1}H} NMR (DMSO-d_6, 100 MHz): δ 173.7, 161.8, 153.7, 153.5, 148.9, 55.4, 55.3, 37.2, 37.1, 33.9, 31.7, 28.8, 25.5, 22.5, 14.6.

By TLC, **S-M** (Rf: 0.7) disappeared and a new spot at Rf 0.0 corresponding to **S-S** indicate all the monomers reacted to form a macrocycle. The ^{1}H NMR spectrum for **S-S** identifies the new

resonances associated with macrocycle synthesis with NNH at 12.51 ppm and A at 7.51 ppm. **S-S** spectrum: ^{1}H NMR (DMSO-d_6, 400 MHZ): δ 12.51 – 12.48 (m, 1H), 11.53 – 11.47 (m, 1H), 8.81 (s, 1H), 7.91 – 7.65 (m, 1H), 7.51 – 7.47 (m, 1H), 4.48 (s, 1H), 4.36 – 4.35 (m, 2H), 3.14 – 3.08 (m, 6H), 2.71 (s, 2H), 2.52 (m, 2H).

Heterodimer Macrocycles. Equal molar amounts of **OA-M** (0.021g, 0.04 mmol) and **S-M** (0.021g, 0.04 mmol) were dissolved in 1 mL of DCM in a vial with a stir bar. Then, 1 mL of TFA was added dropwise slowly. The solution in the vial evaporated over one week within a hood. TLC (10% MeOH in DCM) showed a new spot at Rf: 0.4 in between the **OA-OA** spot (Rf: 0.7) and **S-S** spot (Rf: 0.0). NMR was utilized to verify the synthesis of the heterodimer **OA-S**.

The same procedure was used with equal molar amounts of **OA-M** (0.013g, 0.02 mmol) and **K-M** (0.0128g, 0.02 mmol) to make **OA-K**. This solution took 96 hrs to evaporate. New resonances at 7.2 ppm and 12.3 ppm correspond to the **OA-K** heterodimer, A, and NNH protons. A TLC (10% MeOH in DCM) showed a new spot at Rf: 0.1 in between **OA-OA** (Rf: 0.7) and **K-K** (Rf: 0.0). Added to the crude reaction mixture were N,N-Diisopropylethylamine (0.0649 g, 0.50 mmol), and BOC anhydride (0.0124 g, 0.056 mmol). The BOC group protecting the primary amines are noted as **B**. Thus, the protected **OA-K** and **K-K** are identified by **B OA-K** and **B K-K**. Thin-layer chromatography (5% MeOH in DCM) had a new spot at an Rf: 0.4. ^{1}H NMR verified the synthesis of the heterodimer **OA-K**.

Results and Discussion

NMR Spectrum Conventions. Throughout this thesis, the following conventions are adopted to identify resonances in the NMR spectra (**Chart 2**).

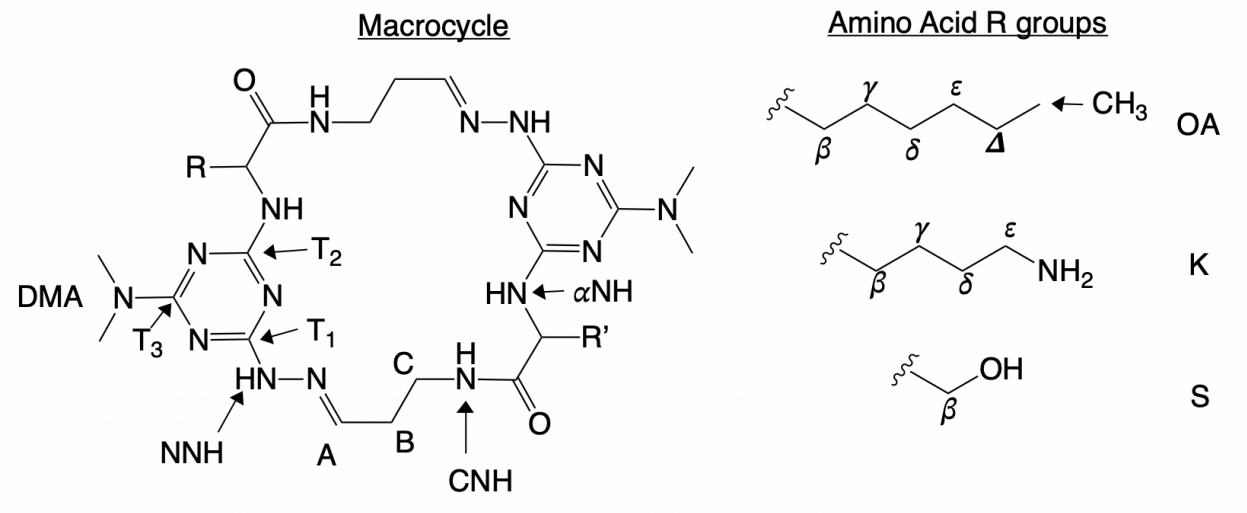

Chart 2. Labeling convention of hydrogens and carbons for NMR spectra.

The labeling system identifies both carbons and protons. The order of the triazine carbons, T_1, T_2, and T_3, reflects the order of nucleophilic addition. DMA notes dimethylamine groups. NNH is used to represent the hydrazine NH. Letters A, B, and C identify the carbons on the acetal, where the most oxidized atom is A. CNH represents acetal amine. αNH represents the amino acid amine. R and R' represent the R groups in the amino acids. In the **X-acid** and **X-M** spectra, BOC is used to identify the *tert-butyl* group on the hydrazine. For **S**, O^{t}Bu represents the *tert-butyl* protecting the 1^o alcohol. The ethoxy groups in the **X-M** spectra are identified as OCH_2CH_3, where the atom of interest is underlined. In the macrocycle spectra, H^+ refers to the triazine ring when protonated. This labeling system will refer to specific resonances in the ^1H or ^{13}C spectra and will be conserved across all species.

Part 1. Synthesis and Characterization of Monomers

*Synthesis of the **X-acid** Derivatives.* Cyanuric chloride undergoes three sequential nucleophilic aromatic substitutions for **X-acid** synthesis. The order of the substitutions is first BOC-hydrazine,

then an amino acid, and finally DMA. The reactivity of the nucleophiles dictates the selection of this order. BOC-hydrazine was used first due to its ease of handling and the beneficial solubility properties of the resulting dichlorotriazine intermediate. BOC-hydrazine was added at 0^{o}C to minimize multiple substitutions of CC.

The addition of amino acids **OA** and **S** to the substituted CC, occurred at room temperature. 2-Aminooctanoic acid was added to the reaction mixture neat because of the reduced reactivity of the dichlorotriazine intermediate and the slow rate of reaction. In addition, **OA** contains a hydrophobic moiety thus it was added neat rather than dissolving it in water. The reaction of **OA** took longer than expected due to the pH of the solution: it was too basic. The primary alcohol on **S** contains a reactive nucleophile that can lead to unwanted side products; thus, for the macrocycle synthesis, the alcohol was protected with a *tert-butyl* group. The mixture had dissolved **S** added to it in one equivalent of water. Dimethylamine was added last in excess.

The three additions of BOC, amino acid and DMA were conducted in the same flask and monitored with TLC. Separating **X-acid** from the side products involved using extraction and silica gel chromatography. The yield of **OA-acid** was 0.247g (30%). Column chromatography of **S-acid** led to a partial purification with the first fractions contaminated with a high Rf impurity. The product has an Rf of 0.5, but the impurities appear at Rf of 0.8. In later fractions, there was 0.094 g of product (Rf: 0.5). The amount of impure **S-acid** recovered was 0.116 g. Thus, the net yield of **S-acid** was 0.210 g (30%).

^{1}H NMR and ^{13}C NMR spectroscopy confirmed the presence of **OA-acid.** ^{1}H NMR spectroscopy confirmed the presence of pure **S-acid**. The three substitutions of BOC-hydrazine, DMA, and the amino acid can all be found on both the ^{1}H NMR spectrum for **OA-acid** (**Figure 2**) and pure **S-acid** (**Figure 3**) in DMSO-d_6. The presence of these three resonances indicates the successful synthesis of the **X-acid**.

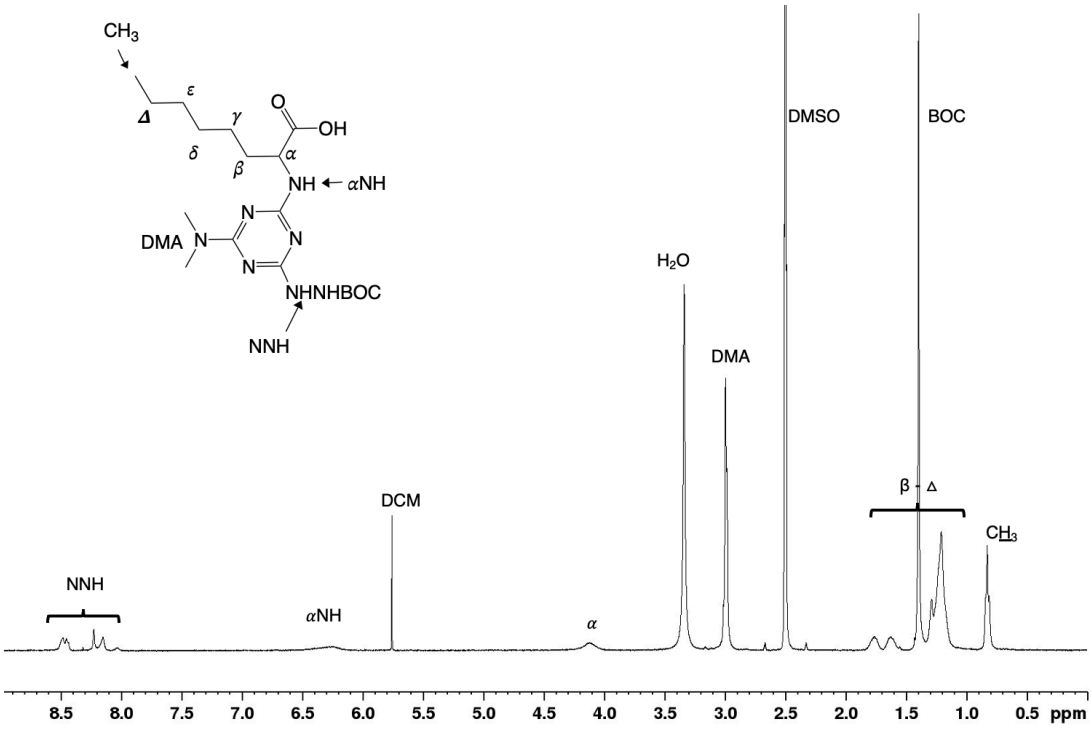

Figure 2. ^{1}H NMR spectrum of **OA-acid** in DMSO-d_6.

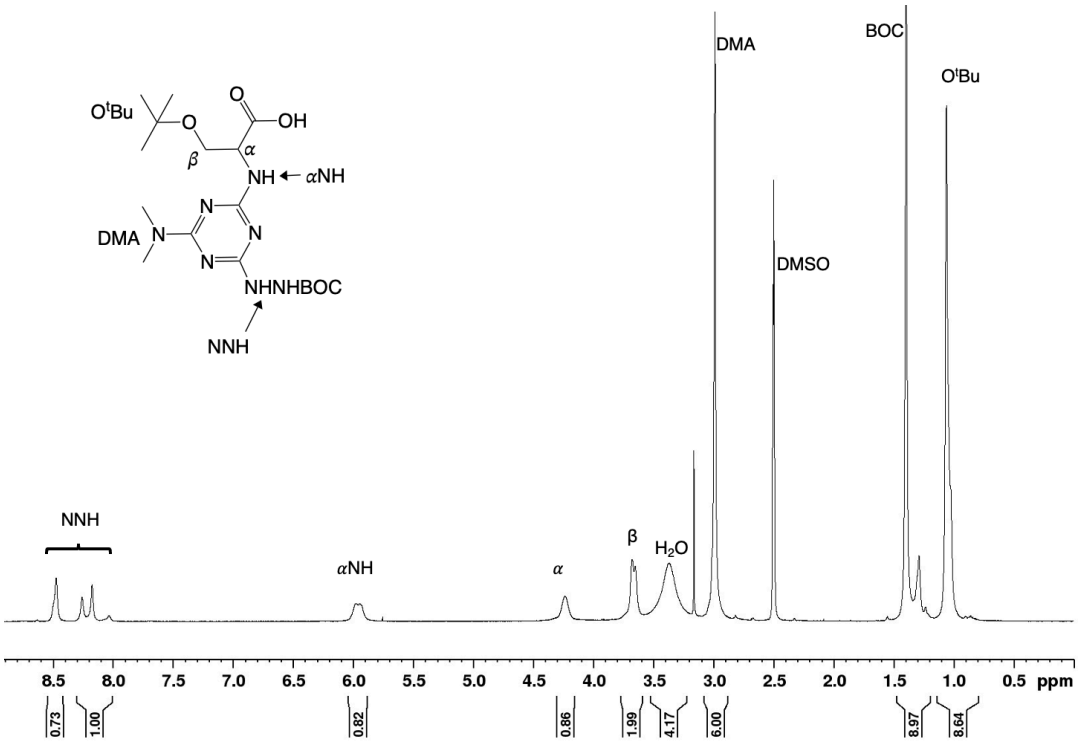

Figure 3. ^{1}H NMR spectrum of **S-acid** in DMSO- d_6.

In **OA-acid**, the amino acid side chain, a long hydrocarbon chain, can be identified as a series of resonances. The α hydrogen appears as a broad resonance at 4.12 ppm. Hydrogens identified as β though Δ appear as resonances in 1.70 ppm to 1.11 ppm regions. A triplet at 0.83 ppm identifies the terminal methyl group. DMA has a resonance at 3.00 ppm. The BOC group appears at 1.70 ppm.

For **S-acid**, the amino acid resonances include the α hydrogen (4.15 ppm) and the β resonances (3.68 ppm). The O^{t}Bu group is at 1.06 ppm in the spectrum, whereas the BOC is at 1.39 ppm. All the resonances corresponding with successful synthesis are present when comparing the two **S-acid** spectra, only pure **S-acid** is shown in this thesis. Deviation between the spectra occurs at two places. The first is a broad resonance past 10 ppm corresponding to the carboxylic acid in the

impure **S-acid**. The second difference is a sharp resonance at 3.14 ppm, corresponding to MeOH. Neither impurity impacts the following steps.

One peculiar feature conserved throughout the **X-acid** spectra are the multiple resonances corresponding to the NNH hydrogen. These multiple resonances appear between 8.0 ppm and 8.5 ppm in all the **X-acid** ^{1}H NMR spectra. The multiple resonances are from the molecule slowly interconverting between conformations in solution. This behavior is not unique and is consistent with the literature and corresponds to the hindered rotation of the triazine-N bond.[12]

Confirmation of the synthesis of **OA-acid** involved obtaining ^{13}C NMR in DMSO-d_6 (**Figure 4**). The carbonyls associated with adding the amino acid and BOC-hydrazine appear at 174.6 ppm and 162.1 ppm, respectively. At 36.6 ppm, resonances belonging to the DMA appear. A mass spectrum was also recorded for **OA-acid,** confirming the product (**Figure S1**). The experimentally determined mass (M_{exp} = 412.2671 Da) matches the predicated mass (M_{pred} = 412.2667 Da) for **OA-acid**.

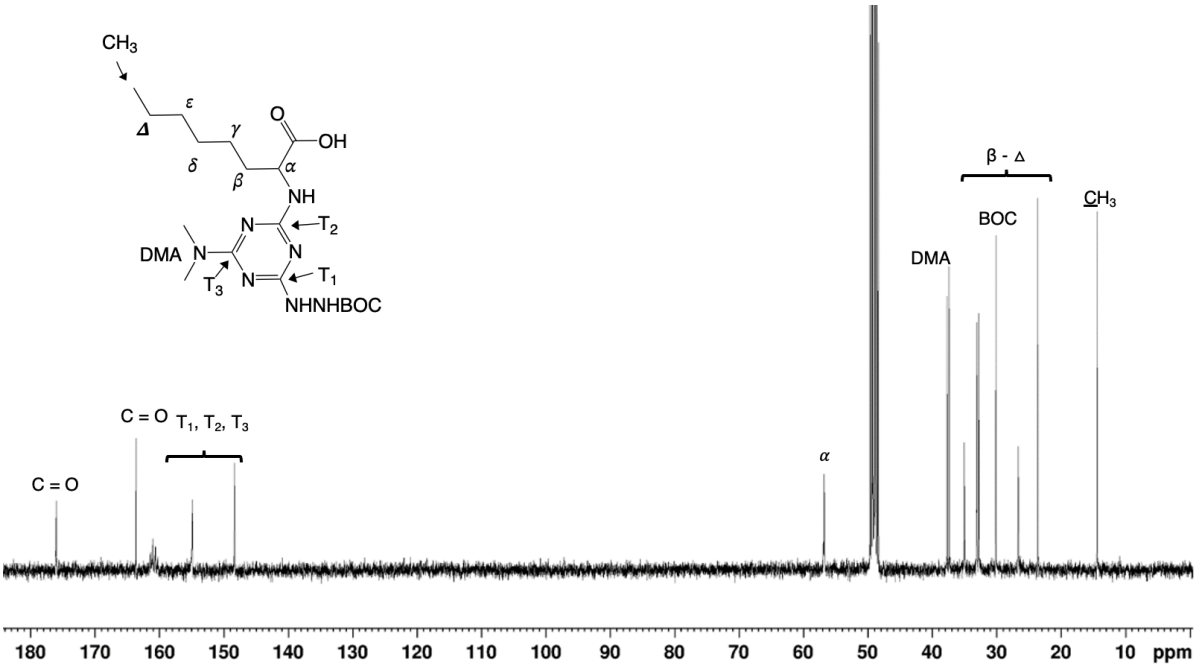

Figure 4. ^{13}C NMR spectrum of **OA-Acid** in DMSO- d_6.

Synthesis of the Monomers. After verification of the successful synthesis of **X-acids**, the acetal groups were added to the compounds using coupling agents HOBT and HBTU. These reagents activate the carbonyl by increasing its electrophilicity and leaving group stability. After separating the reagents into the impure **S-acid** and pure **S-acid**, a TLC was used to track the progression of the reaction. The results exhibited no difference, prompting the combination of results for the remaining reaction steps. After extraction and chromatography, there was a 22 % yield of **S-M** and a 45% yield of **OA-M**.

Confirmation of the synthesis of **OA-M** involved obtaining ^{1}H and ^{13}C NMR spectroscopy in DMSO-d_6 (**Figures 5** and **Figure 6**). Verification of the synthesis of **S-M** involved obtaining ^{1}H and ^{13}C NMR spectroscopy in DMSO-d_6 (**Figures 7** and **Figure 8**).

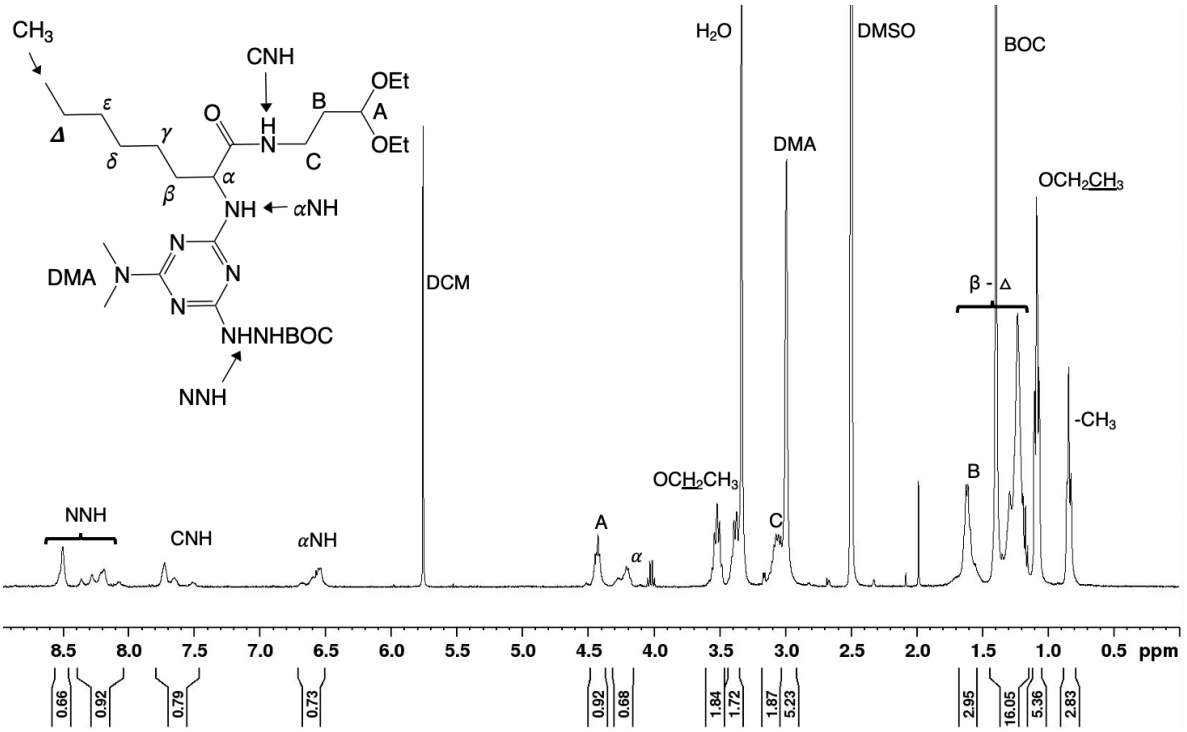

Figure 5. [1]H NMR spectrum of **OA-M** in DMSO-d_6.

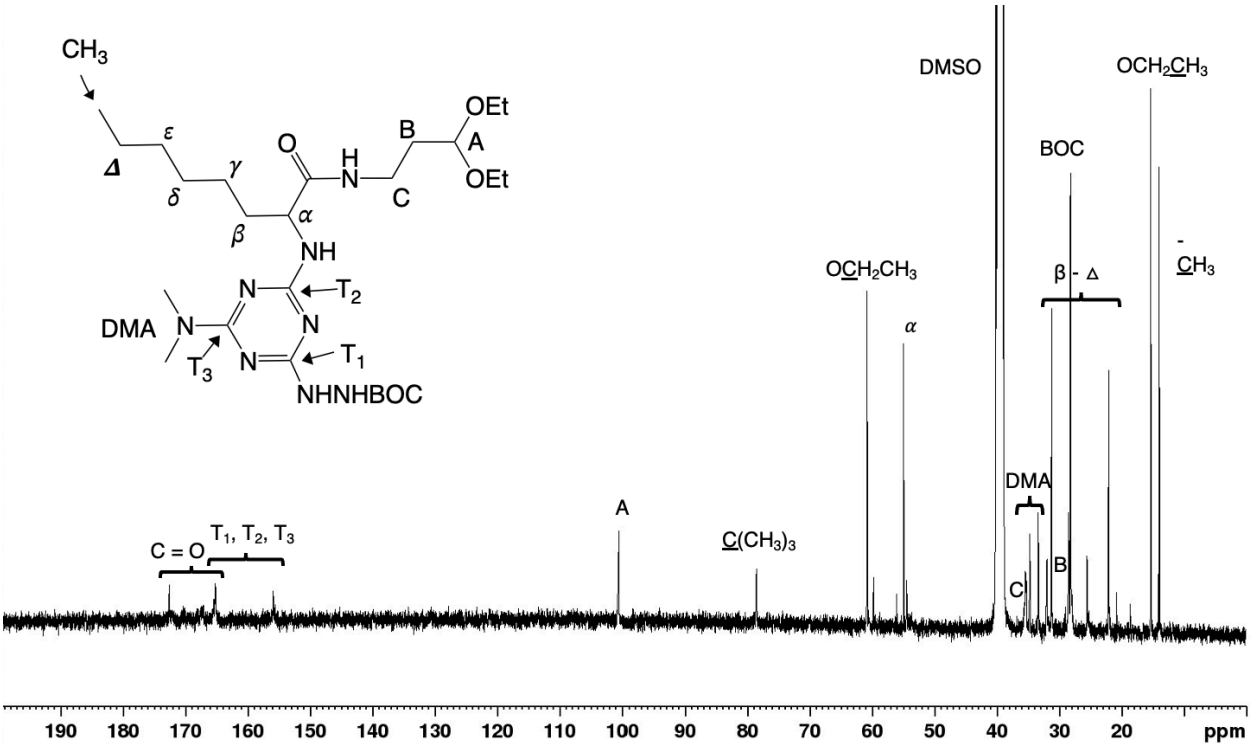

Figure 6. [13]C NMR spectrum of **OA-M** in DMSO- d_6.

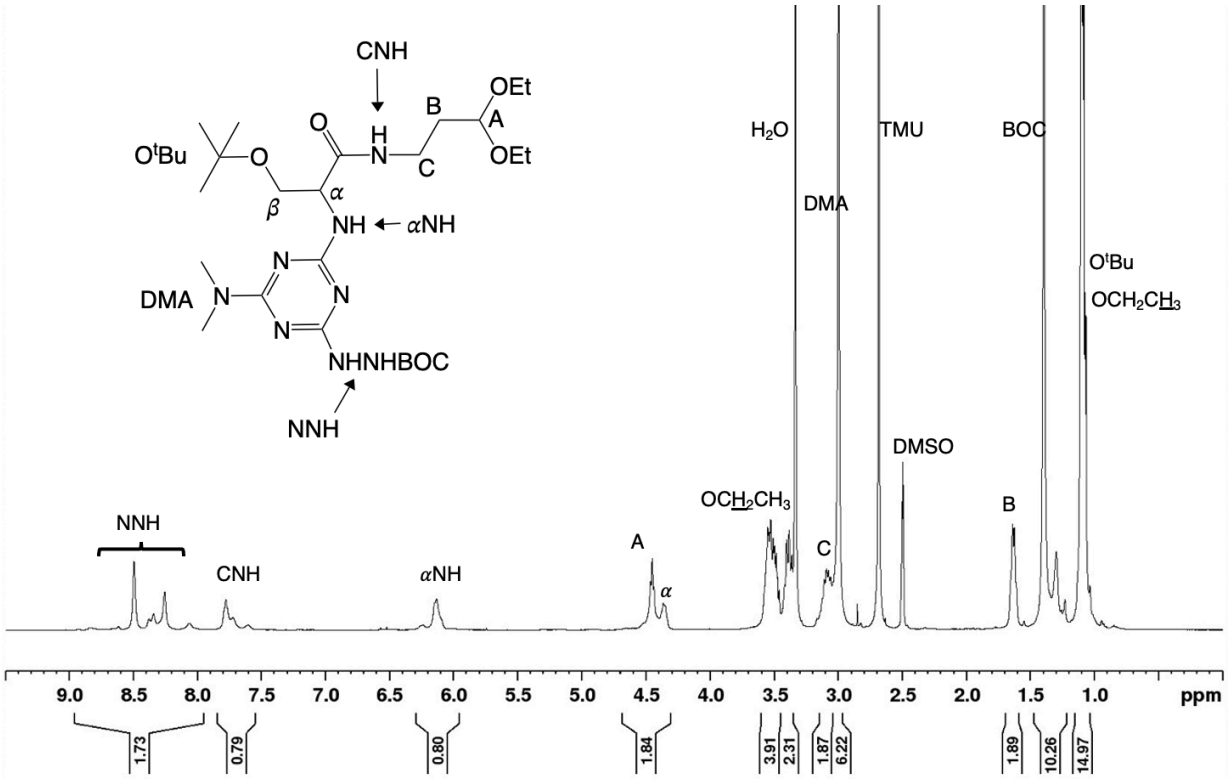

Figure 7. ^{1}H NMR spectrum of **S-M** in DMSO-d_6.

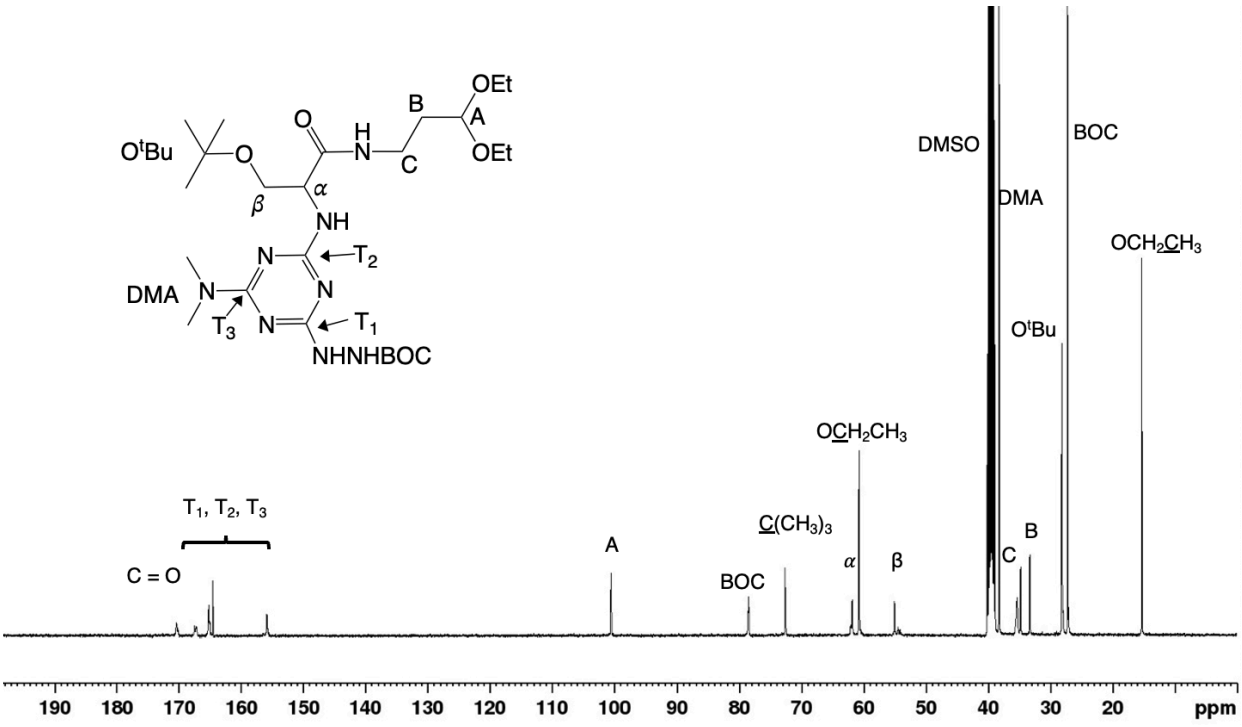

Figure 8. ^{13}C NMR spectrum of **S-M** in DMSO-d_6.

In the ^{1}H spectrum of **OA-M**, the addition of the acetal to **OA-acid** is seen by resonances A, B, and C, which show up at 4.43 ppm, 1.69 ppm, and 3.07 ppm, respectively. The CH_2 group associated with the ethoxy group has two resonances, one at 3.52 ppm and one at 3.37 ppm. The two resonances result from the diastereomeric relationship of the protons. The tetramethyl urea (TMU) impurity appears at 2.66 ppm, but will not impact the following steps. The ^{13}C NMR spectrum for **OA-M** is also consistent, pointing to the synthesis of a monomer. Carbons associated with the acetal have resonances of A at 100.5 ppm, B at 31.2 ppm, and C at 35.4 ppm. A mass spectrum confirmed the **OA-M** synthesis (**Figure S2**). The experimentally determined mass (M_{exp} = 541.3833 Da) matches the predicated mass (M_{pred} = 541.3820 Da) for **OA-M**.

The ^{1}H NMR spectrum of **S-M** shows a similar trend with peaks A, B, and C that indicate the successful addition of acetal to the monomer, 4.46 ppm, 1.64 ppm, 3.11 ppm, respectively. The ethoxy CH_2 resonances appear at 3.55 ppm and 3.41 ppm. The ^{13}C NMR spectrum also show similar findings regarding A, B, and C groups of the acetal. Resonances associated with α and β of **S** are seen at 62.1 ppm and 55.1 ppm, respectively.

Part 2. Synthesis and Characterization of Homodimer Macrocycles

OA-OA *Homodimer.* When **X-M** is added to a 1:1 mixture of TFA to DCM and allowed to evaporate, this method produces a macrocycle without purification. The initial concentration of the **OA-M** was 31.0 mg/mL. Verification of the synthesis of **OA-OA** involved obtaining ^{1}H and ^{13}C NMR spectroscopy.

The ^{1}H NMR for **OA-OA** shows the appearance of the NNH resonance at 12.49 ppm in DMSO-d_6 (**Figure 9**). The NNH peak is the result of the hydrazone formed by condensation of the acetal and the amine groups of two separate monomers. There is only one peak representing two NNH groups due to the symmetry of the macrocycle. The chemical shift of the A peak from 4.43 ppm in the **OA-M** to 7.46 ppm in **OA-OA** represents the new chemical environment associated with the formation of a new bond in the macrocycle. The ^{13}C NMR spectrum is also consistent with macrocycle formation (**Figure 10**). The shift of the A peak from 100.5 ppm to 148.9 ppm confirms the synthesis of the macrocycle. A mass spectrum confirms the synthesis of **OA-OA** (**Figure S3**). The experimentally determined mass (M_{exp} = 697.4861 Da) matches the predicated mass (M_{pred} = 697.4845 Da) for **OA-OA**.

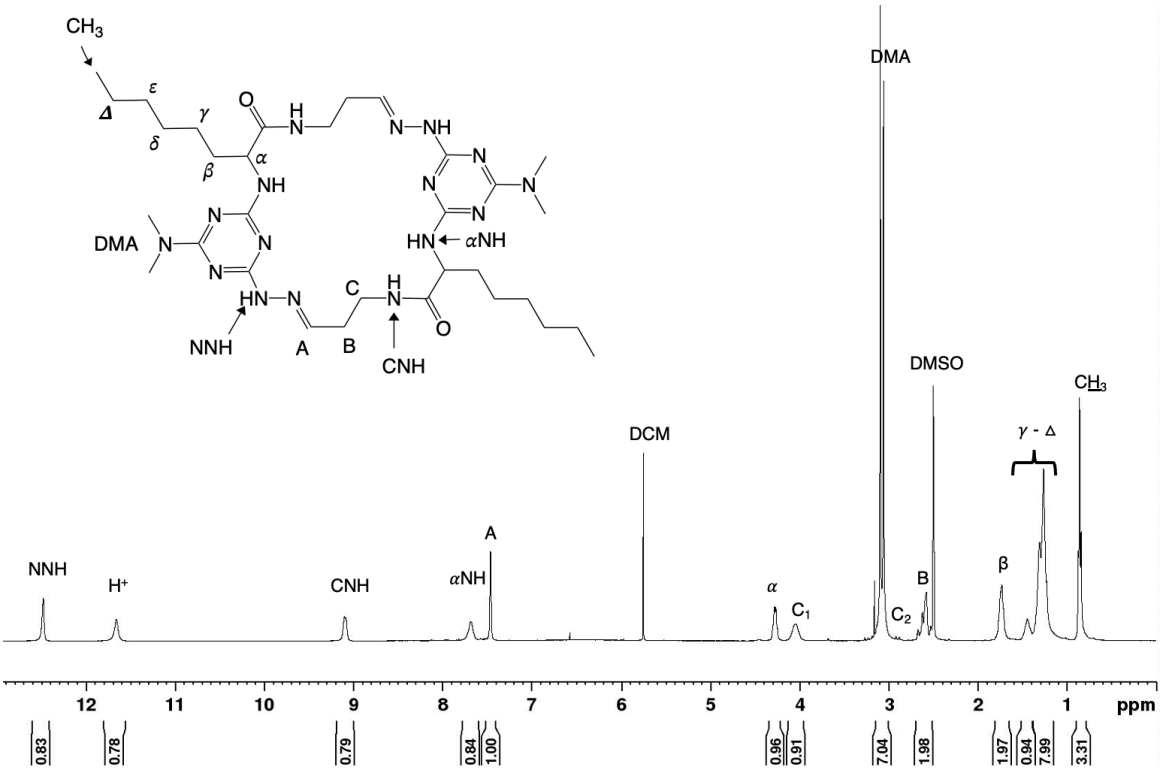

Figure 9. ^{1}H NMR spectrum of **OA-OA** in DMSO-d_6.

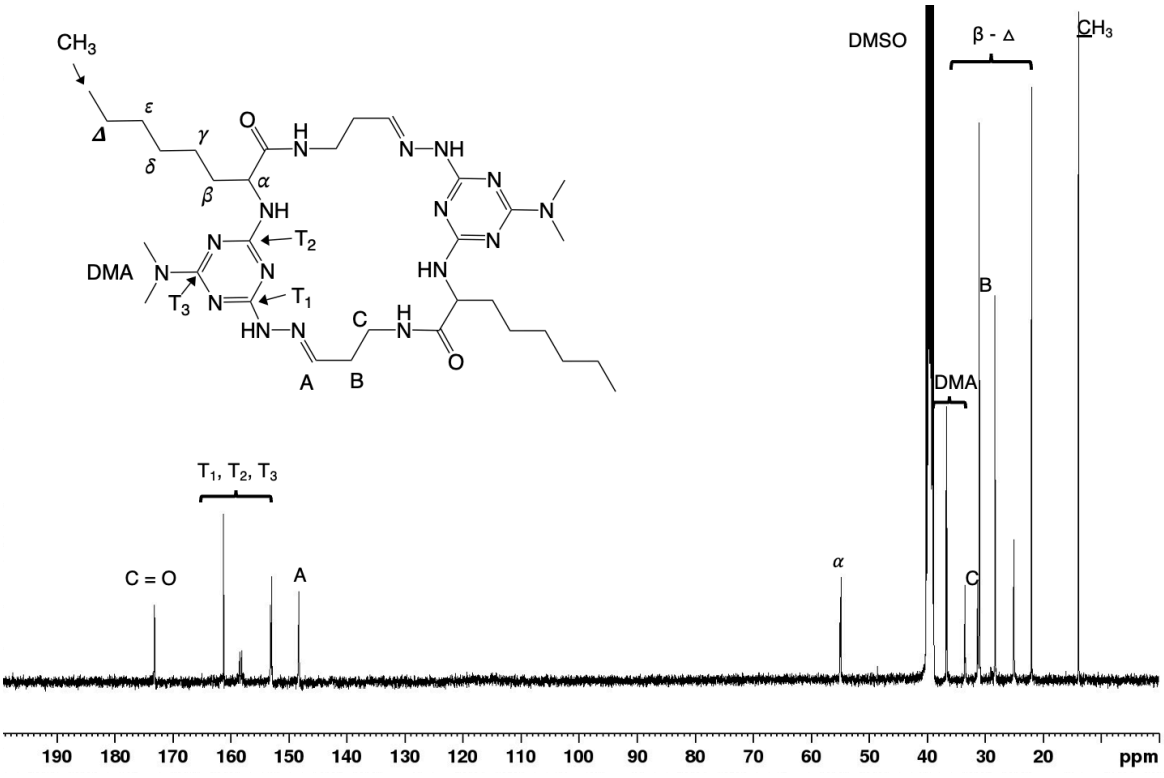

Figure 10. ^{13}C NMR spectrum of **OA-OA** in DMSO-d_6.

S-S *Homodimer.* The concentration in the **S-M** homodimer reaction was initially 8.95 mg/mL. Confirmation of the **S-S** macrocycle synthesis involved obtaining ^{1}H NMR spectroscopy in DMSO-d_6. The ^{1}H NMR spectrum for **S-S** also shows the presence of the NNH resonance at 12.51 ppm and A at 7.51 ppm (**Figure 11**). Instead of a single resonance, each resonance in the up-field region exists as multiples. A possible explanation of the resonances existing as multiples could be due to the *tert-butyl* group protecting the primary alcohol being cleaved by the acidic induced environment of TFA into 2-methylpropene and leaving the hydroxyl group which can undergo an elimination reaction, leaving a terminal double bond. Since the double bond is planar, water can attack the terminal end from either plane, creating a racemic product. When this happens to the macrocycle, it creates different stereoisomers, each with unique resonances. The broad peak at 3.8 ppm is excess acidic water within the sample.

The [1]H NMR spectrum for **K-K** was provided by Alex Menke, and is shown in **Figure 12**.

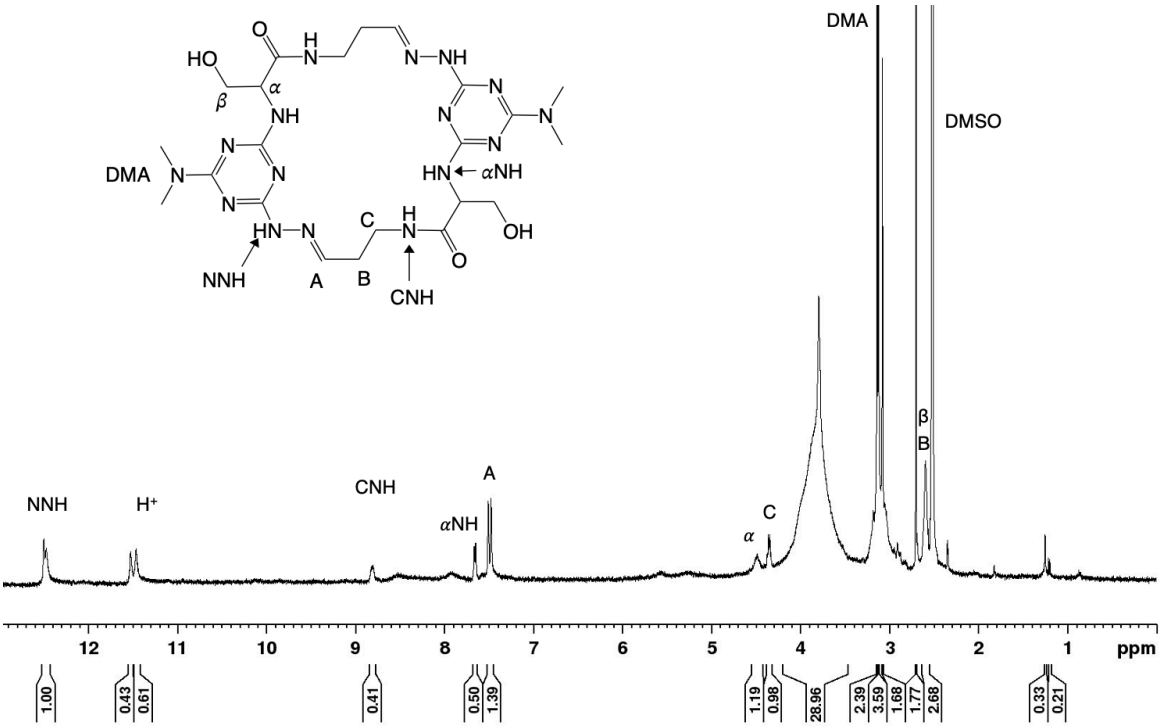

Figure 11. [1]H NMR spectrum of **S-S** in DMSO-d_6.

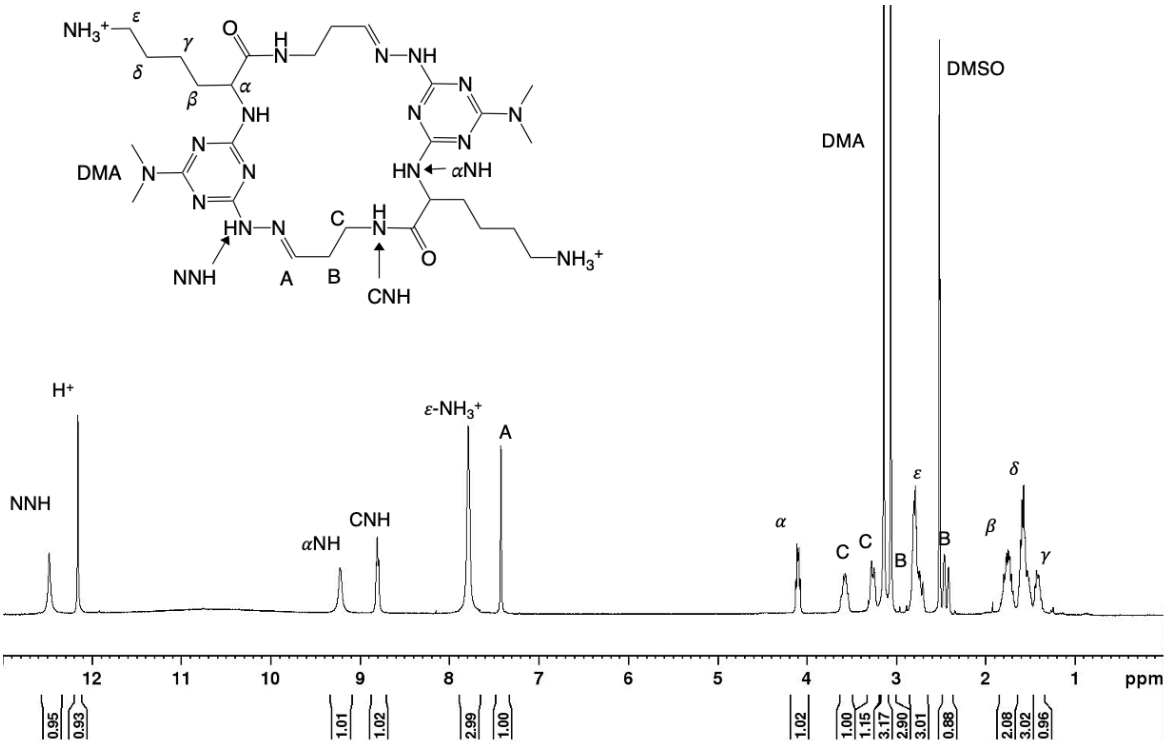

Figure 12. ^{1}H NMR spectrum of **K-K** in DMSO-d_6.

Part 3. Synthesis and Characterization of Heterodimer Macrocycles

OA-S *Heterodimer.* Equal molar parts of **OA-M** to **S-M** were added to a 1:1 mixture of TFA and DCM and evaporated until dry. The initial concentration of the monomers was 21 mg/mL. A comparison between the corresponding homodimers and crude **OA-S** reaction mixture, which contains **OA-OA**, **OA-S**, and **S-S,** reveals the presence of the heterodimer. The ^{1}H NMR spectra showed new resonances that indicate heterodimer synthesis (**Figure 13**). A "new" H^+ resonance appears at 11.5 ppm for **OA-S**, 9.2 ppm for CNH, and 7.2 ppm for A. Using column chromatography to separate the heterodimer from the homodimers was unsuccessful.

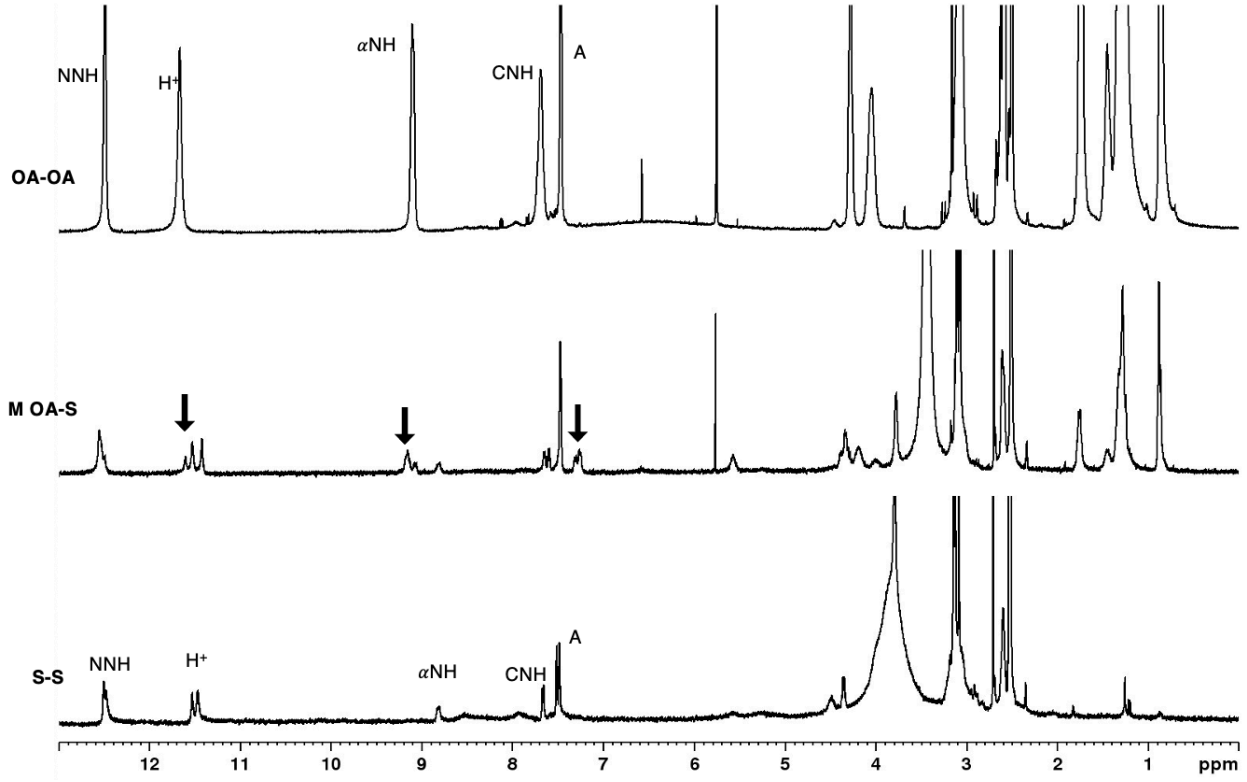

Figure 13. Stacked plot ^{1}H NMR spectra of **OA-OA**, **OA-S**, and **S-S** in DMSO-d_6. Arrows indicate presence of novel peaks in reaction mixture (M **OA-S**) corresponding to synthesis of **OA-S** macrocycle.

OA-K *Heterodimer.* The synthesis of **OA-K** followed the same process as **OA-S**. Equal molar amounts of **OA-M**:**K-M** was dissolved in DCM: TFA (1:1). The concentration of the monomers was 13 mg/mL. Resonances at 7.2 ppm and 12.3 ppm correspond to the **OA-K** heterodimer A and NNH protons (**Figure 14**). The new resonance at 4.2 ppm could correspond to C or α, and further experimentation will be needed to isolate and confirm the structure.

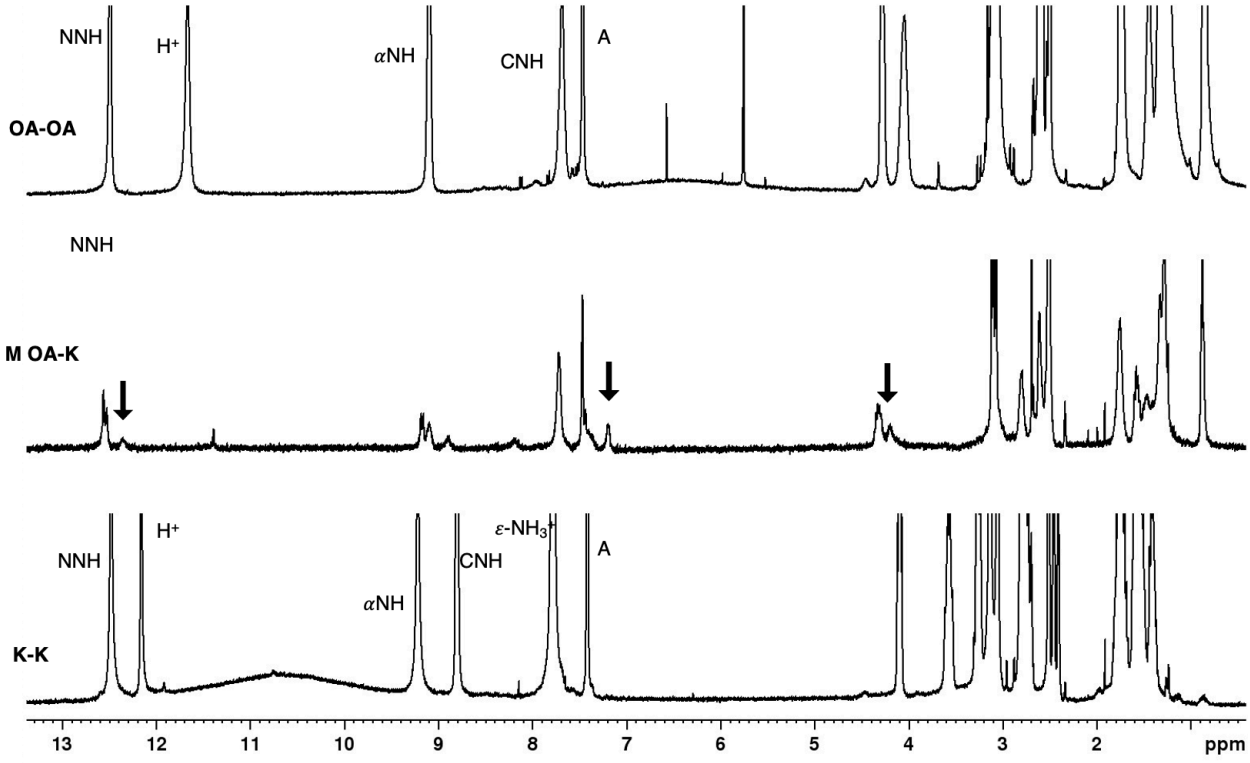

Figure 14. Stacked plot ^{1}H NMR spectra of **OA-OA**, **OA-K**, and **K-K** in DMSO-d_6. Arrows indicate presence of novel peaks in reaction mixture (M **OA-K**) corresponding to synthesis of **OA-K** macrocycle.

Part 4. Shape Characterization of the Macrocycle OA-OA

A homonuclear correlation spectroscopy, COSY, identifies the neighboring hydrogens on adjacent carbons (i.e., 2, 3, and sometimes 4 bonds apart). A COSY spectrum was obtained for **OA-OA** (**Figure 15**). Upon identifying the A hydrogen, it "sees" the B proton because they are on adjacent carbons. Verifying α to both β and αNH is accomplished using the same method.

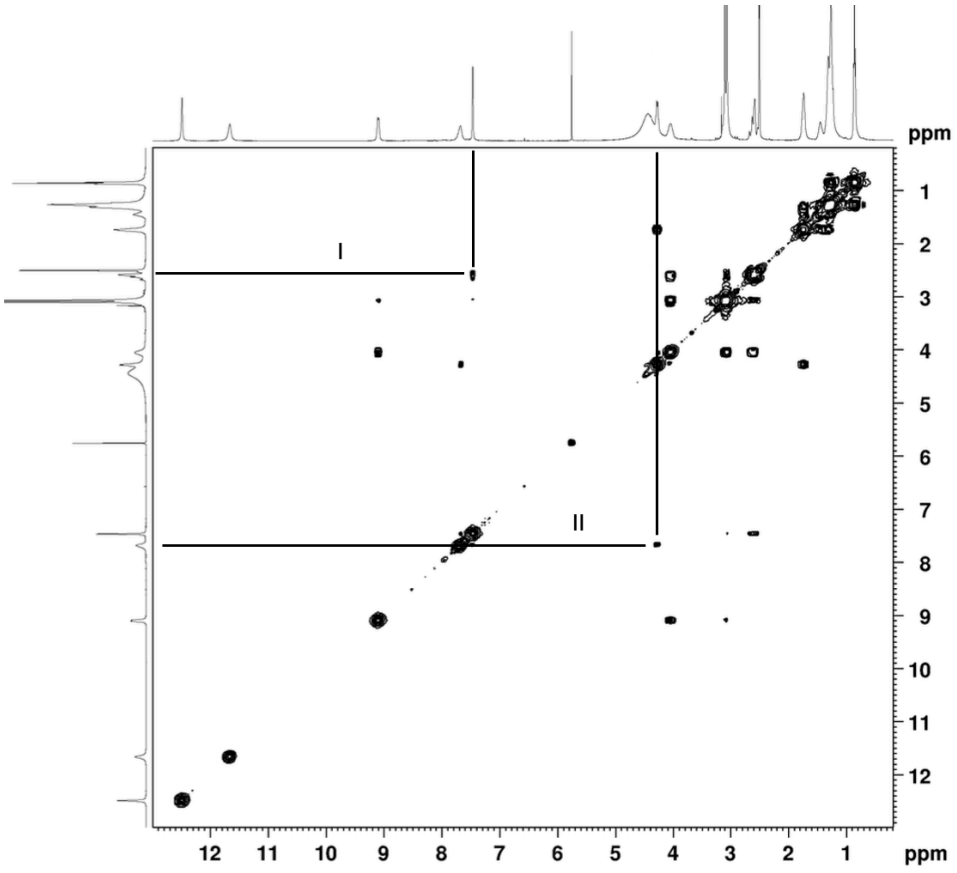

Figure 15. ^{1}H x ^{1}H COSY spectrum of the macrocycle, **OA-OA** in DMSO-d_6. I) coupling of A hydrogen to B hydrogens on acetal. II) coupling of α to β and α to αNH.

A rotating frame Overhauser effect spectroscopy experiment, rOsey, produces signals from protons that are close in space. This spectrum provides information regarding the 3D shape of the macrocycle. A rOsey was recorded for **OA-OA** DMSO-d_6 (**Figure 16**). We know the macrocycle has a folded morphology due to a correlation between A and DMA. In the structure, these protons are far from each other and do not appear in a COSY. The rOsey establishes the *E*-hydrazone stereochemistry of the hydrazone because of the correlation between A and the NNH proton. The orientation of the αNH is towards the center of the macrocycle because it sees the H^+ associated with the triazine ring. Lacking a peak associated with the H^+, we infer that the orientation of the NNH hydrogen is away from the center of the macrocycle.

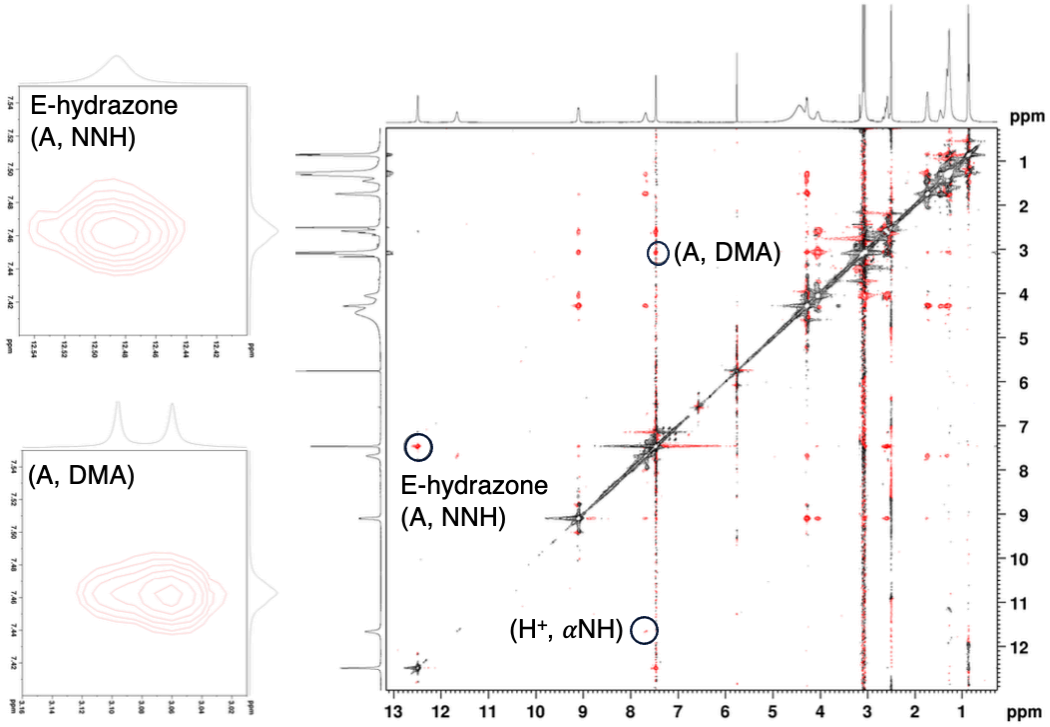

Figure 16. The rOsey NMR spectrum of **OA-OA** in DMSO-d_6, identifies a folded structure, (A, DMA), *E*-hydrazone orientation of the double bond, (A, NNH), and inward orientation of αNH (H^+, αNH).

Part 5. Assessing the Polarity of the Heterodimers.

Thin-Layer Chromatography. A TLC experiment was performed after the heterodimer **OA-S** mixture fully evaporated (**Figure 17**). A novel spot in the crude reaction mixture appeared at Rf: 0.4. This spot is at the intermediate distance between **OA-OA** (Rf: 0.7) and **S-S** (Rf: 0.0). The intermediate spot corresponds to the **OA-S** heterodimer. The hydrophobic domain **OA** sidechain pulled the polar group of **S** off the baseline in the heterodimer.

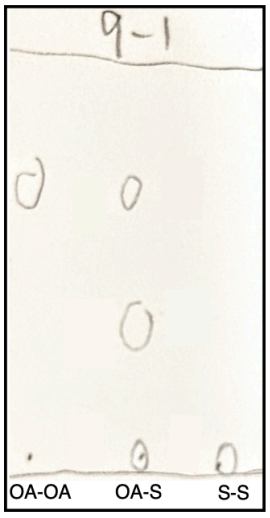

Figure 17. TLC (10% MeOH to DCM) identifies a novel spot at Rf: 0.4 that corresponds to **OA-S** heterodimer. The reaction conditions employed leads to the simultaneous production of **OA-OA**, **OA-S** and **S-S** as seen in the lane marked **OA-S**.

The TLC for the **OA-K** reaction mixture shows a new spot that minimally moved off the baseline (**Figure 18**). The Rf of **OA-K** was 0.1. BOC-anhydride masked the amines of the **OA-K** and **K-K**, to yield **B OA-K** and **B K-K.** The TLC of this reaction mixture showed that all the spots migrated off the baseline (**Figure 19**).

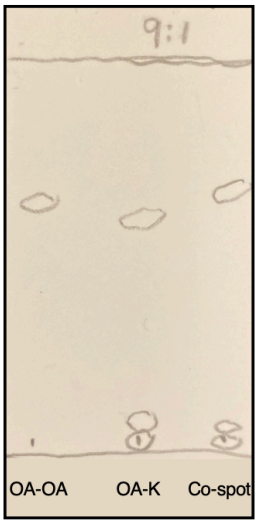

Figure 18. TLC (10% MeOH to DCM) identifies shows a novel spot at Rf: 0.1 corresponds to **OA-K** heterodimer. The reaction conditions employed leads to the simultaneous production of **OA-OA**, **OA-K** and **K-K** as seen in the lane marked **OA-K**.

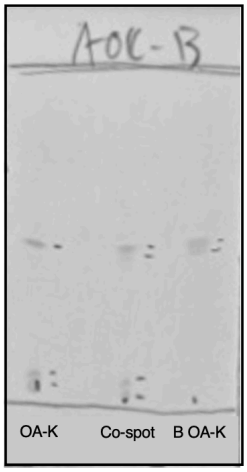

Figure 19. TLC in 5% MeOH to DCM shows movement of all protected amines in **B OA-K** and **B K-K** off the baseline to Rf 0.4.

Reverse Phase-High Performance Liquid Chromatography. A series of selected standards underwent RP-HPLC analysis to ascertain the logP values of the **B OA-K** reaction mixture. These standards' Rt were transformed into k-values by subtracting the lysine Rt (the dead volume

standard) from it and then dividing the lysine Rt. Subsequently, the logarithm of the k-values was calculated, yielding the logK values. Crafting a graphical representation by plotting the previously determined logP values for the standards against the logK values established a correlation that can be employed to determine logP values of other compounds (**Graph 1**). Values for all standards are seen in the supporting information (**B OA-K** standards **Chart S1**, **OA-S** standards **Chart S2**). Using linear regression on **Graph 1** provided the equation for the line of best fit with a R^2 value of 0.992. This equation was then utilized to determine the logP values for the **B OA-K** reaction mixture (**Table 1**).

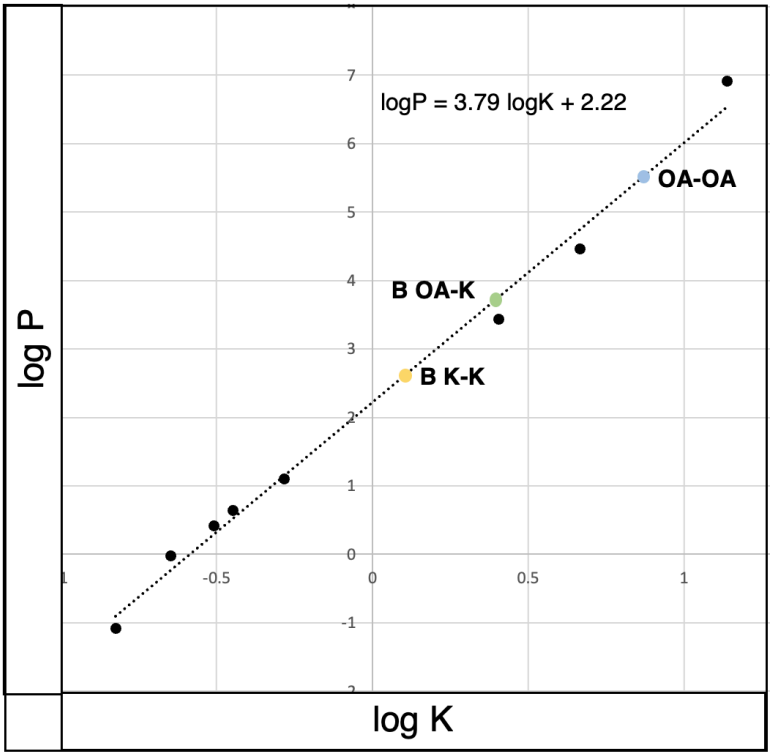

Graph 1. The plot of standard logP and experimentally determined logK provides an equation that gives logP values to **OA-OA** (5.4), **B OA-K** (3.8), and **B K-K** (2.6).

Macrocycle	Rt (min)	k-value	logK	logP
OA-OA	10.553	6.881	0.837668	5.4
B OA-K	4.855	2.625	0.419268	3.8
B K-K	2.996	1.237	0.092542	2.6

Table 1. Rt, k-value, logK and logP determined for **OA-OA**, **B OA-K**, and **B K-K** from RP-HPLC experimentation.

From the measured data the lowest logP of 2.6, which belongs to **B K-K**, corresponds to the fastest partitioning macrocycle through the column due to hydrophilic side groups not interacting as much with the solid phase. The logP of **OA-OA** was 5.4. This logP was the highest value and corresponds to the slowest partition though the column due to the hydrophobic side chains interacting with the column. Heterodimer **B OA-K** has a logP of 3.8, which is between the two homodimers but closer in value to **B K-K** then **OA-OA**.

When a molecule is ionized based on the pH of the solution, the partition coefficient is reported as logD instead of logP. The same method that was used for **B OA-K** was used to determine the logD for **OA-OA**, **OA-S**, and **S-S** (**Graph 2** and **Table 2**). Here, instead of lysine Rt being subtracted it was the dead time for serine. The R^2 value for the line of best fit was 0.994.

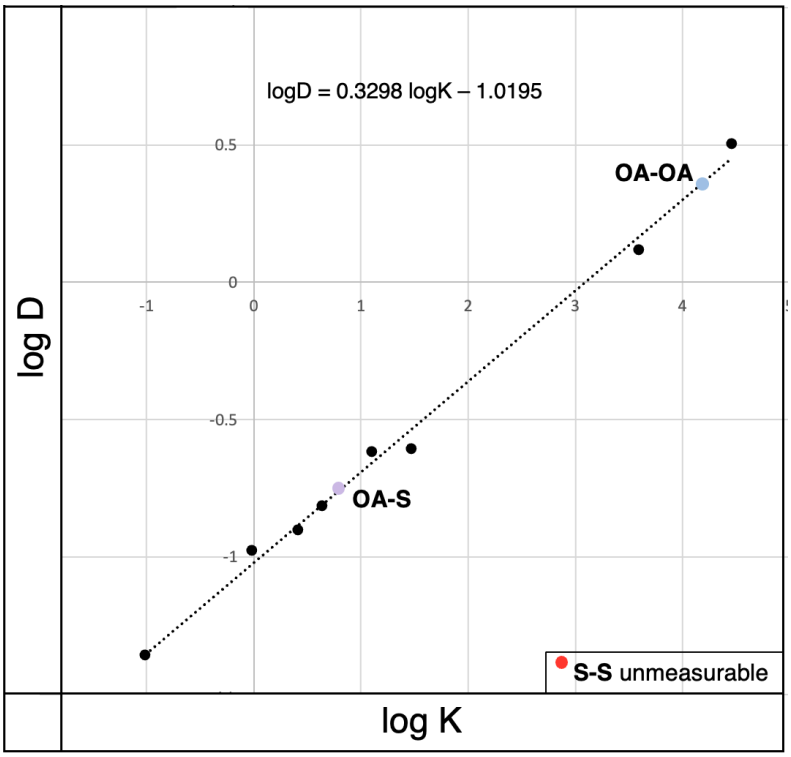

Graph 2. The plot of standard logD and experimentally determined logK provides an equation that gives logD values to **OA-OA** (4.2), **OA-S** (0.8), and **S-S** (< -2.2).

Macrocycle	Rt (min)	k-value	logK	logD
OA-OA	6.523	2.422	0.384	4.2
OA-S	2.246	0.178	-0.748	0.8
S-S	1.903	-1.57×10^{-3}	error	< -2.2

Table 2. Rt, k-value, logK and logD determined for **OA-OA**, **OA-S**, and **S-S** from RP-HPLC experimentation.

Homodimer **S-S** partition out of the column the fastest due to the high polarity of the primary alcohol groups. Since **S-S** partitioned out so fast, it has an unmeasurable value represented by logD < -2.2. Homodimer **OA-OA** had a logD value of 4.2.[13] Again, similar to the logP, it had the largest

value due to the interactions with the stationary phase that made it have a slow Rt. The hydrocarbon chain of **OA** in the heterodimer was enough to have a measurable logD value of **OA-S** at 0.8.

Conclusion

Shape is critical for function. A correct arrangement of atoms is essential for drugs to have a therapeutic effect. This work details preserving a constant macrocycle shape while simultaneously engineering another crucial property of drugs: the prediction of their membrane-crossing ability. Changing the amino acid resulted in a change in the chemical property. The homodimers offer extremes of polarity with **OA-OA** being hydrophobic (logP 5.4; logD 4.2; TLC Rf: 0.7), while **S-S** (logD: <-2.2; TLC Rf: 0.0) and **K-K** (Rf: 0.0) represent the hydrophilic extreme. All of these molecules adopt a similar shape.

By synthesizing heterodimers, we have shown that molecules with intermediate polarities can be observed in **OA-K** (Rf: 0.1) and **OA-S** (logD: 0.8; Rf: 0.4). Moreover, when the addition of a BOC protecting group reduces the polarity. The behavior of the new molecule **B OA-K** (logP: 2.6; Rf: 0.4) still follows this trend. 2-Aminooctanoic acid contributes to making **K** and **S** more hydrophobic compared to homodimers. This ability to mask polar amino acids or potential functional groups that might be critical for drug action with nonpolar ones to help shepherd the molecule across the membrane holds promise for expanding possibilities in drug synthesis. Future research will focus on isolating these heterodimers to validate their synthesis, potentially paving the way for pharmaceutical companies to explore novel approaches for creating orally available drugs.

Supporting Information

Chart 1S. logP, Rt, k-value and logK values for **OA-OA**, **B OA-K**, and **B K-K** standards.

Standards	logP	rt	k	logK
Lysine	---	1.339	---	---
thiourea	-1.08	1.539	0.149365	-0.82575
theophylline	-0.02	1.64	0.224795	-0.64821
furfural	0.41	1.752	0.308439	-0.51083
pyrrole-2-carboxaldehyde	0.64	1.817	0.356983	-0.44735
benyzl alcohol	1.1	2.033	0.518297	-0.28542
p-dichlorobenzene	3.44	4.738	2.538462	0.404571
phenanthrene	4.46	7.534	4.626587	0.665261
DDT	6.91	19.687	13.70276	1.136808

Chart 2S. logP, Rt, k-value and logK values for **OA-OA**, **OA-S**, and **S-S** standards.

Standards	LogD	rt (min)	k-value	LogK
Serine	---	1.906	---	---
thiourea	-1.01	1.99	0.044071	-1.35584
theophylline	-0.02	2.107	0.105456	-0.97693
furfural	0.41	2.145	0.125393	-0.90172
pyrrole-2-carboxaldehyde	0.64	2.199	0.153725	-0.81326
benyzl alcohol	1.1	2.367	0.241868	-0.61642
phenanthrene	4.46	7.988	3.190976	0.503924
phenylbenzoate	3.59	4.402	1.309549	0.117122
phenol	1.47	2.38	0.248688	-0.60434
doxorubicin	1.27	2.398	0.258132	-0.58816

Figure S1. The HRMS (ESI) spectrum for **OA-acid**.

Elmt	Val.	Min	Max	Elmt	Val.	Min	Max	Elmt	Val.	Min	Max	Elmt	Val.	Min	Max	Use Adduct
H	1	1	200	O	2	0	4	P	3	0	0	I	3	0	0	H
B	3	0	0	F	1	0	0	S	2	0	0	Ir	3	0	0	
C	4	18	18	Na	1	0	0	Cl	1	0	0					
N	3	0	7	Si	4	0	0	Br	1	0	0					

Error Margin (ppm): 100
HC Ratio: unlimited
Max Isotopes: all
MSn Iso RI (%): 75.00

DBE Range: -2.0 - 1000.0
Apply N Rule: yes
Isotope RI (%): 1.00
MSn Logic Mode: AND

Electron Ions: both
Use MSn Info: no
Isotope Res: 10000
Max Results: 500

Event#: 1 MS(E+) Ret. Time : 0.313 -> 0.333 Scan# : 48 -> 51

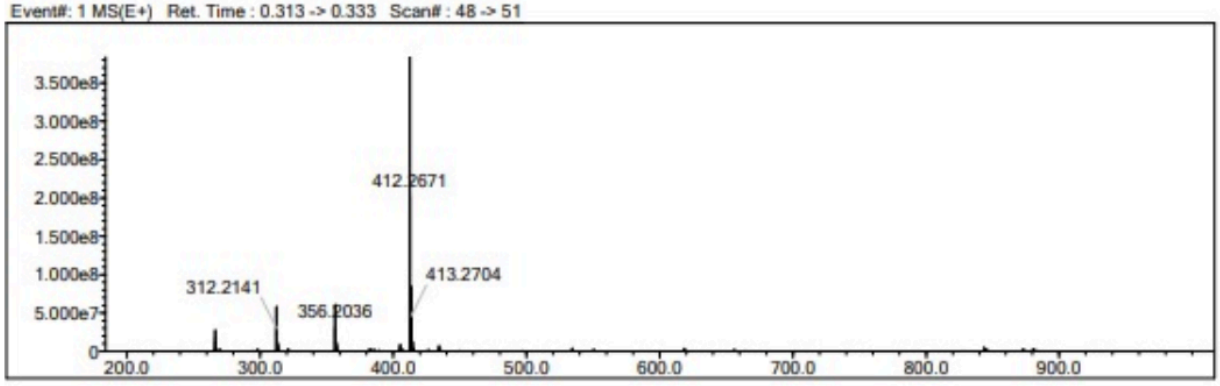

Measured region for 412.2671 m/z

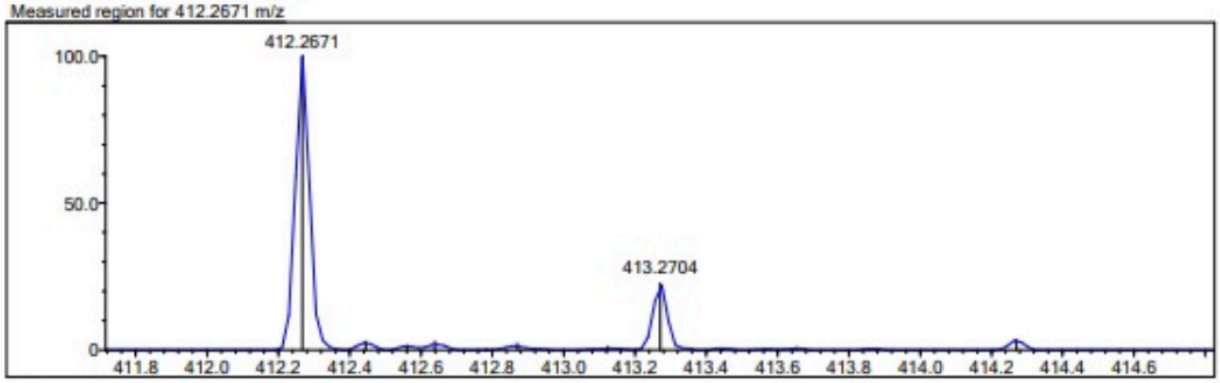

C18 H33 N7 O4 [M+H]+ : Predicted region for 412.2667 m/z

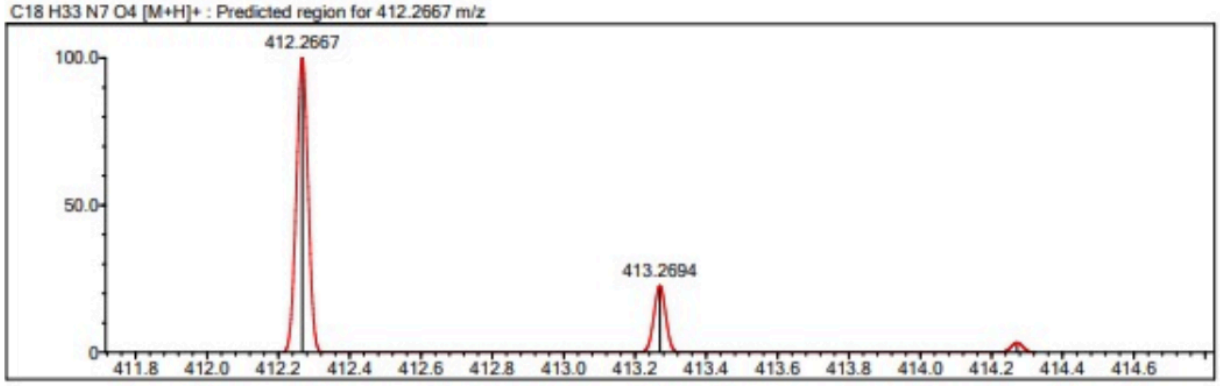

Rank	Score	Formula (M)	Ion	Meas. m/z	Pred. m/z	Df. (mDa)	Df. (ppm)	Iso	DBE
1	100.00	C18 H33 N7 O4	[M+H]+	412.2671	412.2667	0.4	0.97	100.00	6.0

Figure S2. The HRMS (ESI) spectrum of **OA-M**.

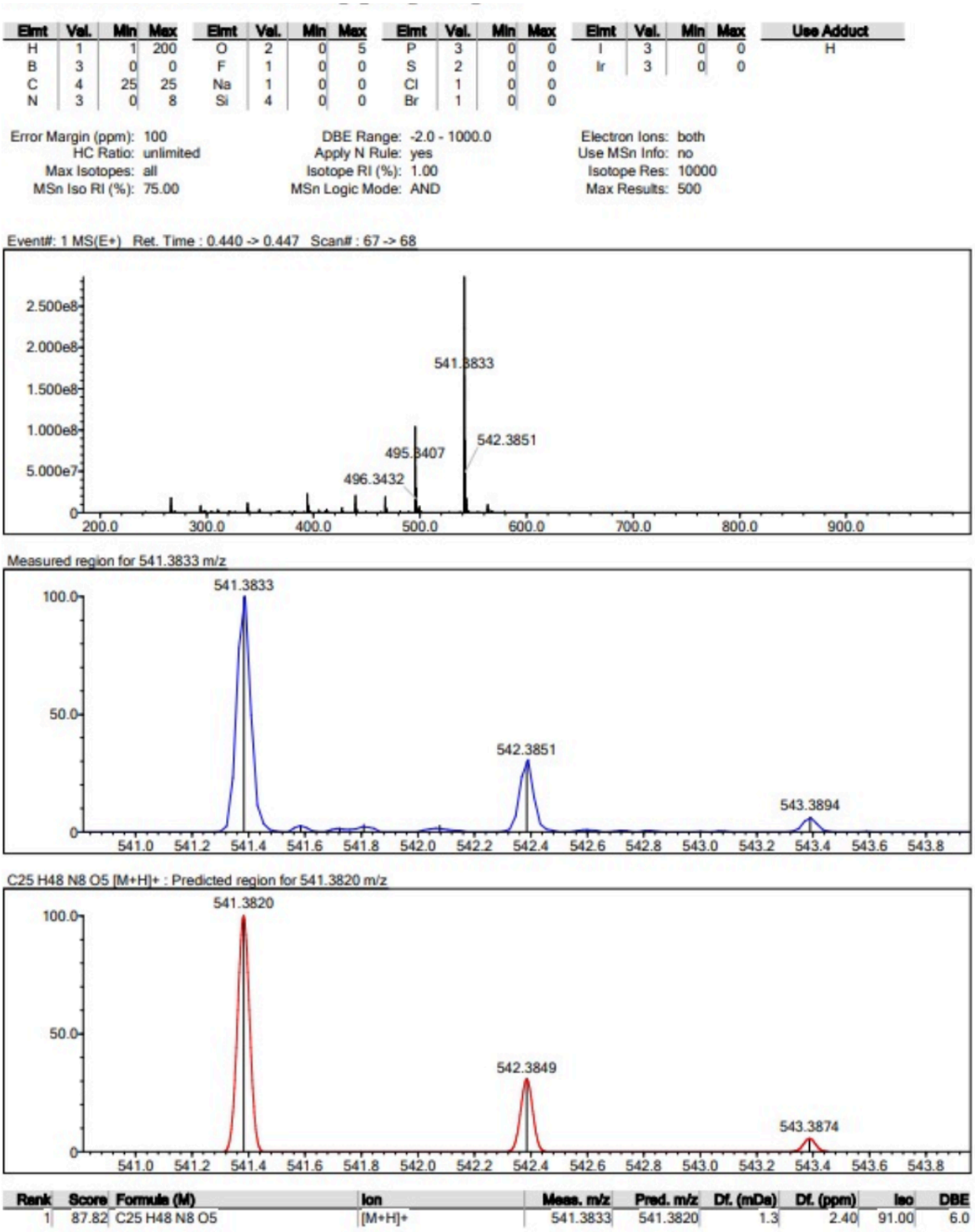

Figure S3. The HRMS (ESI) spectrum of **OA-OA.**

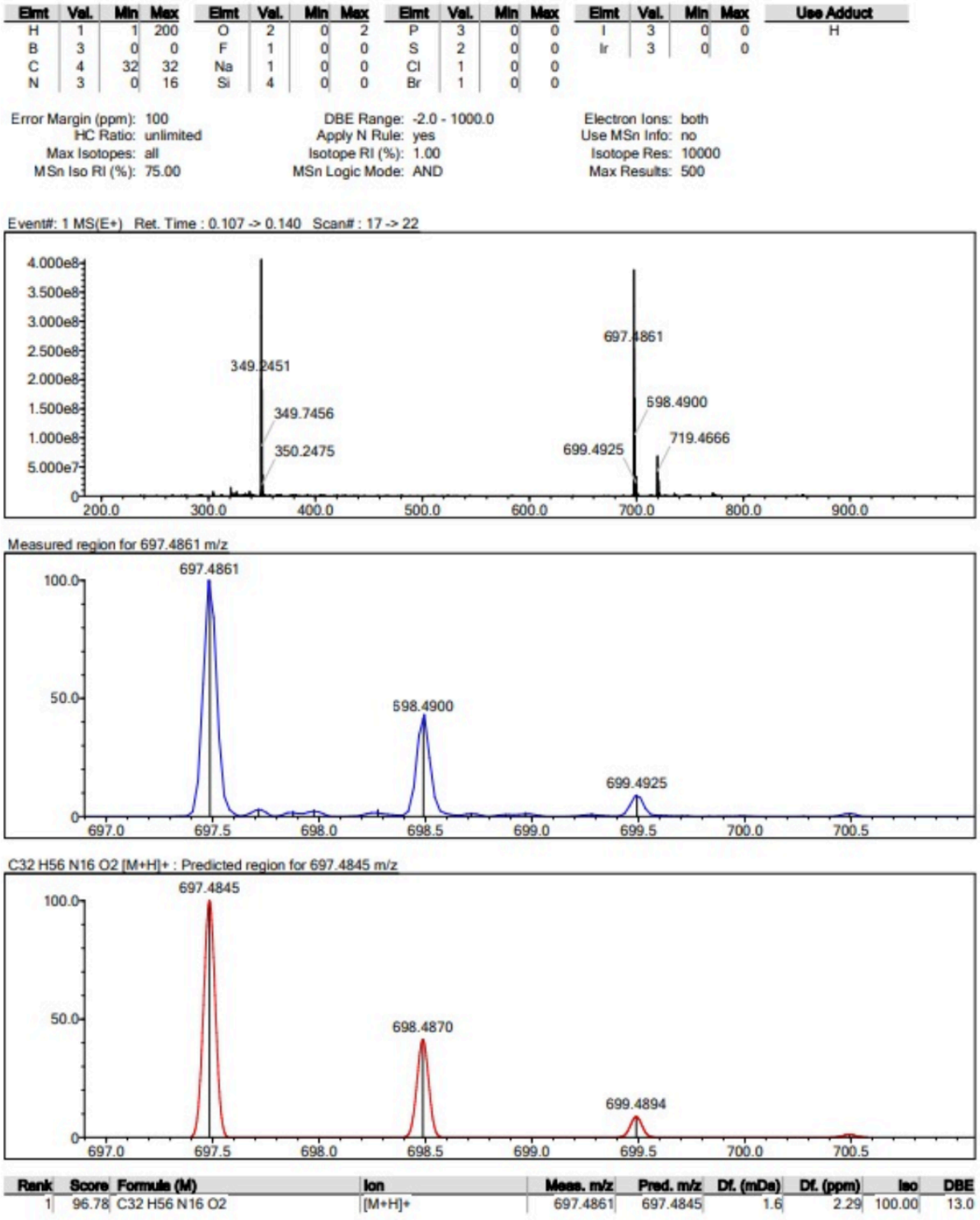

References

1. Lin, L.; Wong, H. Predicting Oral Drug Absorption: Mini Review on Physiologically-Based Pharmacokinetic Models. *Pharmaceutics* **2017**, *9* (4), 41. https://doi.org/10.3390/pharmaceutics9040041.

2. Gupta, U.; Perumal, O. Dendrimers and Its Biomedical Applications. *Natural and Synthetic Biomedical Polymers* **2014**, 243–257. https://doi:10.3389/fphar.2021.618411

3. Alqahtani MS, Kazi M, Alsenaidy MA, Ahmad MZ. Advances in Oral Drug Delivery. Front Pharmacol. **2021** Feb 19;12:618411. doi: 10.3389/fphar.2021.618411. PMID: 33679401; PMCID: PMC7933596.

4. Lipinski, C. A.; Lombardo, F.; Dominy, B. W.; Feeney, P. J. Experimental and Computational Approaches to Estimate Solubility and Permeability in Drug Discovery and Development Settings. *Adv. Drug Deliv. Rev.* **2012**, *64*, 4–17. https://doi.org/10.1016/j.addr.2012.09.019.

5. Kirkpatrick, P. Chris Lipinski. Interview. *Nat. Rev. Drug Disc.* **2012**, *11* (12), 900–901. https://doi.org/10.1038/nrd3895.

6. Croy Doak, B.; Over, B.; Giordanetto Jan, F.; Kihlberg. Oral Druggable Space beyond the Rule of 5: Insights from Drugs and Clinical Candidates. *Chem. & Biol.* **2014**, *21* (9), 1115–1142. https://doi.org/10.1016/j.chembiol.2014.08.013.

7. Yudin, A. K. Macrocycles: Lessons from the Distant Past, Recent Developments, and Future Directions. *Chem. Sci.* **2015**, *6* (1), 30–49. https://doi.org/10.1039/c4sc03089c.

8. Tapia C, Nessel TA, Zito PM. Cyclosporine. [Updated 2023 Mar 7]. In: StatPearls [Internet]. Treasure Island (FL): StatPearls Publishing; **2023** Jan. Available from: https://www.ncbi.nlm.nih.gov/books/NBK482450/

9. Yepremyan, A.; Mehmood, A.; Asgari, P.; Janesko, B. G.; Simanek, E. E. Synthesis of Macrocycles Derived from Substituted Triazines. *ChemBioChem* **2018**, *20* (2), 241–246. https://doi.org/10.1002/cbic.201800475

10. Menke, A.J.; Henderson, N.C.; Kouretas, L.C.; Estenson, A.N.; Janesko, B.G.; Simanek, E.E. Computational and Experimental Evidence for Templated Macrocyclization: The Role of a Hydrogen Bond Network in the Quantitative Dimerization of 24-Atom Macrocycles. *Molecules* **2023**, *28*, 1144. https://doi.org/10.3390/molecules28031144

11. Ghose, A. K.; Viswanadhan, V. N.; Wendoloski, J. J. A Knowledge-Based Approach in Designing Combinatorial or Medicinal Chemistry Libraries for Drug Discovery. 1. A Qualitative and Quantitative Characterization of Known Drug Databases. *J. Comb. Chem.* **1999**, *1* (1), 55–68. https://doi.org/10.1021/cc9800071.

12. Bentz, W. E., Colebrook, L. D., Fehlner, J. R., Rosowsky, A. Hindered rotation about C-N bonds: equilibration of diastereomeric rotational isomers. *J. Chem. Soc. D*, **1970**, (16), 974-974. https://doi.org/10.1039/c29700000974.

13. Patterson-Gardner, C.; Pavelich, G. M.; Cannon, A. T.; Simanek , E. E. Adaptation of Empirical Methods to Predict the LogD of Triazine Macrocycles. *ACS Med. Chem. Lett.* **2023**, 14(10), 1378 – 1382. https://doi.org/10.1021/acsmedchemlett.3c00290.